REC-ERC-78-2

HYDRAULIC LABORATORY MANNING'S *n* AND GRADE DEVIATION STUDY FOR 4-INCH-DIAMETER NONPERFORATED, CORRUGATED PLASTIC DRAIN TUBING

Engineering and Research Center

Bureau of Reclamation

February 1978

MS-230 (1-76)
Bureau of Reclamation

TECHNICAL REPORT STANDARD TITLE PAGE

1. REPORT NO. REC-ERC-78-2	2. GOVERNMENT ACCESSION NO.
3. RECIPIENT'S CATALOG NO.	
4. TITLE AND SUBTITLE Hydraulic Laboratory Manning's *n* and Grade Deviation Study for 4-inch-diameter Nonperforated, Corrugated Plastic Drain Tubing	5. REPORT DATE February 1978
	6. PERFORMING ORGANIZATION CODE
7. AUTHOR(S) E. R. Zeigler	8. PERFORMING ORGANIZATION REPORT NO. REC-ERC-78-2
9. PERFORMING ORGANIZATION NAME AND ADDRESS Engineering and Research Center, Bureau of Reclamation, Denver CO 80225	10. WORK UNIT NO.
	11. CONTRACT OR GRANT NO.
	13. TYPE OF REPORT AND PERIOD COVERED
12. SPONSORING AGENCY NAME AND ADDRESS Same	14. SPONSORING AGENCY CODE

15. SUPPLEMENTARY NOTES

16. ABSTRACT

Laboratory tests were made with an 18-m (60-ft) long, 100-mm (4-in) diameter, nonperforated plastic drain tube. Probes for measuring the static head were 2.4-mm (3/32-in) diameter and placed at 1.8-m (6-ft) intervals along the tube. Tests were made for full-tube flow and free-surface flow at 0.001, 0.005, 0.01, and 0.02 tube slopes. The test results are given in graphs of average velocity and discharge versus uniform depth. Manning's *n* was approximately 0.016. Grade deviations were studied with bends. Four bends, 2.4 m (8 ft) long, with one- and two-tube diameter offsets above and below grade, were tested. There was a significant rise in the hydraulic gradeline upstream from the bend only with bends above grade and for conditions of free-surface flow. A fine, uniform 0.2-mm mean diameter sand was used for sedimentation tests. For flow conditions with a 0.001 slope and a two-diameter tube offset bend below grade, the sediment did not prevent waterflow through the bend.

17. KEY WORDS AND DOCUMENT ANALYSIS

a. DESCRIPTORS-- / *subsurface drains/ hydraulics/ fluid flow/ steady flow/ subcritical flow/ *discharge (water)/ *flow resistance/ hydraulic gradient/ *water surface profiles/ *bends/ sedimentation/ deposition/ erosion/ bed movements

b. IDENTIFIERS-- / nonperforated, corrugated plastic drain tubing

c. COSATI Field/Group 13/K *COWRR:* 1311

18. DISTRIBUTION STATEMENT *Available from the National Technical Information Service, Operations Division, Springfield, Virginia 22151.*	19. SECURITY CLASS (THIS REPORT) *UNCLASSIFIED*	21. NO. OF PAGES 55
	20. SECURITY CLASS (THIS PAGE) *UNCLASSIFIED*	22. PRICE

REC-ERC-78-2

HYDRAULIC LABORATORY MANNING'S *n* AND GRADE DEVIATION STUDY FOR 4-INCH-DIAMETER NONPERFORATED, CORRUGATED PLASTIC DRAIN TUBING

by

E. R. Zeigler

February 1978

Hydraulics Branch
Division of Research
Engineering and Research Center
Denver, Colorado

SI METRIC

UNITED STATES DEPARTMENT OF THE INTERIOR * BUREAU OF RECLAMATION

ACKNOWLEDGMENTS

The study was a cooperative effort by the ARS (Agricultural Research Service) and USBR (Bureau of Reclamation). The test program was suggested by Dr. Lyman Willardson, ARS, and Mr. Ray Winger, Chief of the Drainage and Groundwater Branch, USBR. Mr. Timothy Laraway, Rotation Engineer, assisted in a portion of the laboratory study.

CONTENTS

Page

Purpose 1
Introduction 1
Conclusions 1
Application 3
Test facility 3
Straight tube tests 3

Full-tube flow 3
Free-surface tube flow 9

Introduction 9
Method of performing the tests 9
Test results 10

Bend tests 11

Introduction 11
Constant-flow depth tests 11
Full-tube flow bend losses 15
Other flow depth tests 17
Observations of air entrapment 21

Sedimentation tests 22

Introduction 22
Sediment injection procedure 23
General characteristics of sediment movement 23
Pyramid sediment deposit 25
Lengthwise sediment deposit 25
Sediment deposit in the 2DB bend 31

Appendix 1—Tables 33

1—Results of the full-tube flow tests 35
2—Invert elevations and related manometer board invert readings 36
3—Results of an individual free-surface tube flow test 37
4—Results of the free-surface tube flow tests 37
5—Manometer readings for bend tests at the 0.001 test slope 41
6—Head differences ΔH for bends above grade 42
7—Adjusted head differences for the 2DA and 2DB bends, $S \approx 0.005$ test slope 43

Appendix 2—Entrapped air 45
Appendix 3—Sedimentation tests 49

FIGURES

Figure		Page
1	Effect of grade deviation upon subsurface drainage	2
2	The corrugated plastic tubing installed on the tilting flume	4
3	Test facility	4
4	Static head probes	5
5	Tubing dimensions	6
6	The four test bends	7
7	Friction factor for full-tube flow	8
8	Mannings *n* versus average velocity for full-tube flow	8
9	Velocity versus slope for full-tube flow	9
10	Comparison of test slopes obtained by two-point method and least squares fit	10
11	Schematic showing relation of manometer reading to water depth	10
12	Uniform depth versus average velocity	11
13	Uniform depth versus discharge	12
14	Uniform depth versus Manning's *n*	13
15	Uniform depth versus Manning's *n* comparison for test slopes	13
16	Schematic showing graphical distortion of bend	13
17	Hydraulic gradelines for bend tests, $S = 0.001$	14
18	Hydraulic gradelines for bend tests, $S = 0.005$	15
19	Hydraulic gradelines for bend tests, $S = 0.020$	16
20	Photographs showing water surface profiles in the bends, $S = 0.001$	18
21	Hydraulic gradelines for 2DA bend, $S = 0.005$	19
22	Water surface profiles in the 2DA bend, $S = 0.005$	20
23	Head difference versus discharge, bends 2DA and 2DB, $S = 0.005$	21
24	Hydraulic gradelines for 2DB bend, $S = 0.005$	22
25	Water surface profiles in the 2DB bend, $S = 0.005$	23
26	Cyclic movement of air within the 2DA bend	24
27	Sieve analysis of sedimentation sand	25
28	Schematic showing template method for measuring sediment depth	25
29	Sedimentation tests with a pyramid-shaped sediment deposit	26
30	Sedimentation tests with a lengthwise sediment deposit	27
31	Schematic showing distance of sediment movement for the lengthwise sediment deposit tests	28
32	Hydraulic gradelines for lengthwise sediment deposit	28
33	Sedimentation tests in the 2DB bend	29
34	Shapes of the sediment deposit in the tube downstream from the 2DB bend	30
35	Hydraulic gradelines for 2DB bend sediment deposit test	31
36	Water surface profiles, 2DB bend, $S = 0.001$	46
37	Head difference versus operation time in the 2DB bend, $S = 0.005$	46

PURPOSE

This study was to measure Manning's *n* in 100-mm (4-in) diameter corrugated plastic drain tubing for full-tube and free-surface flow, determine hump and sag alinement effects upon flow in the tubing, and determine whether sediment deposition would obstruct flow in the tubing.

INTRODUCTION

The use of corrugated plastic tubing for subsurface drains is increasing rapidly throughout the world. In the United States alone, millions of lineal meters are installed annually. Because the tubing is flexible and lightweight, long lengths can be conveniently handled and easily installed. The tubing has promoted the use of newer high-speed installation methods.

Small grade deviations may occur in drainlines for a number of reasons. Unstable soils may allow the drains to shift during backfilling operations. Operator error may cause deviations from the planned gradeline. Connections at intersection points of lateral and collector lines may be higher or lower than expected. These grade deviations can cause hydraulic conditions that may reduce the efficiency of the drain system.

Field drains can operate as closed conduits or as open channels where the hydraulic gradeline corresponds to the water surface elevation inside the tube. Thus, a vertical bend in the tube above the gradeline can raise the hydraulic gradeline upstream from the bend; the effective drainage depth below ground surface is reduced accordingly (fig. 1). Also, vertical bends, either upward or downward, change flow velocities upstream from and in the bend, which in turn affects the transport and deposition of soil particles in the water. Knowledge of the effects of vertical bends is therefore important for drainage design.

When establishing drain installation specifications, the drainage engineer must determine what magnitude of grade deviation is acceptable. Excessively strict grade requirements will increase installation costs. Research under controlled laboratory conditions can help determine effects of vertical grade deviation upon waterflow, hydraulic gradelines, and sediment movement. To provide these kinds of information, a cooperative program was initiated by the ARS (Agricultural Research Service) and USBR (Bureau of Reclamation), with the test facility being located in the hydraulic laboratory of the USBR, Engineering and Research Center in Denver, Colo.

The scope of the test program was influenced by a number of factors: The test facility should be constructed so the drain tubing could be raised or lowered to make deviations from grade while a steady waterflow passes through the tubing. Sufficient hydraulic measurements should be made to determine Manning's *n* and from which to compute theoretical backwater curves for comparison with experimentally determined water surfaces. Measurements should include tube slope, depth of flow in the tube, flow rate, water temperature, water surface profile, and the sediment deposition profile. Make observations of flow instabilities and air entrapment produced by the bends.

CONCLUSIONS

1. For full-tube flow, the *n* value for the 100-mm (4-in) diameter nonperforated polyethylene plastic corrugated tubing was 0.015 to 0.016.

2. For free-surface flow, *n* varied from 0.015 to 0.018. High *n* values occurred for high- and low-flow depths, and low *n* values between one-fourth and three-fourths flow depths.

3. For full-tube flow, the hump and sag bends with a one- and two-diameter offset from grade had a negligible effect upon hydraulic gradeline elevations.

4. For free-surface flow, the sag bends had a negligible effect upon hydraulic gradeline elevations, but hump bends raised the hydraulic gradeline elevation upstream from the bend. This rise in elevation was approximately equal to the bend offset distance, and it would reduce drainage depth between parallel drains by that offset distance. At the downstream end of the bend, there was a hydraulic jump, and with discharge increases, the jump contacted the top of the tubing. Thereupon, air was flushed from the bend which produced a siphoning effect

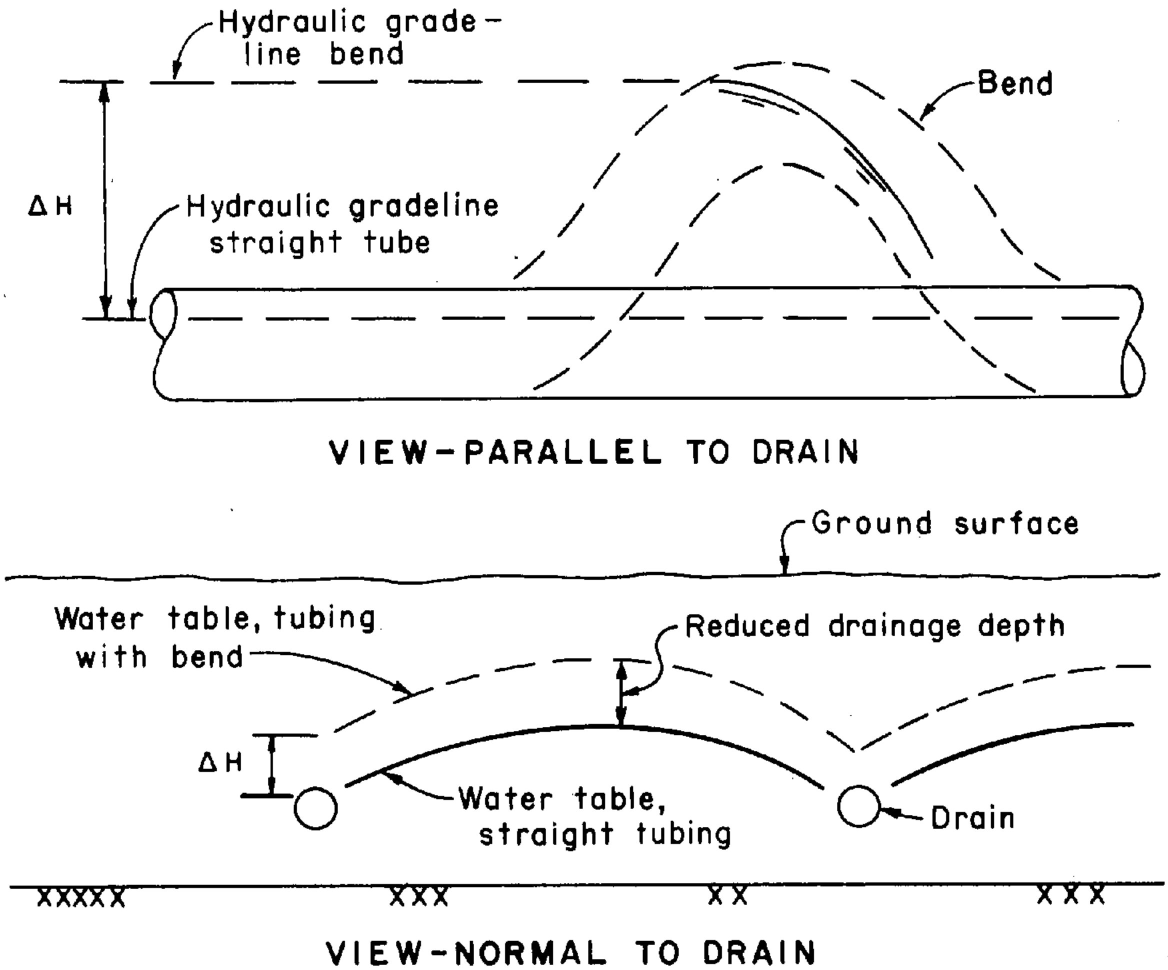

Figure 1.–Effect of grade deviation upon subsurface drainage.

within the bend and a lowering of the upstream hydraulic gradeline.

5. Sedimentation tests were made with a uniform grade sand of 0.2-mm mean diameter. For full-tube flow, a velocity of 0.12 m/s (0.4 ft/s) produced incipient sediment movement: a velocity of 0.24 m/s (0.8 ft/s) moved sediment 0.6 m/h (2 ft/h), a velocity of 0.31 m/s (1.0 ft/s) moved sediment 1.2 m/h (4 ft/h), a velocity of 0.36 m/s (1.2 ft/s) moved sediment 3.7 m/h (12 ft/h), and a velocity of 0.67 m/s (2.2 ft/s) rapidly flushed sediment from the tube corrugations.

6. Sedimentation tests were made at a 0.001 tube slope and a two-diameter offset sag bend. At low discharges, the bend nearly filled with sediment; however, waterflow through the tube did not stop and there appeared to be a nonclogging tendency. As the cross-sectional area of the sediment deposit increased, the flow velocity above the deposit also increased until it became sufficient to transport the sediment. With progressively increased discharges, more of the sediment deposit was removed from the bend.

7. Tubing used in the laboratory tests was nonperforated and may have reacted differently than a perforated field drain. Siphoning which occurred in the laboratory tests may not occur in the field because of air admittance. Also, water in a field drain may leave the tubing and flow into the surrounding gravel envelope, producing different sediment behavior within a

bend. Thus, the laboratory test results should be cautiously interpreted when applied to drain installation specifications.

8. Future research, both in the laboratory and field, is needed to determine siphoning and sedimentation characteristics of bends with perforated tubing.

APPLICATION

The study results provide an accurate *n*-value for design purposes. Furthermore, results of *n*-variation with free-surface flow will give designers information for making theoretical backwater studies.

Care should be used in applying short-time operation and laboratory length drain tests to field conditions of 50- to 100-year operation and long lengths. Nevertheless, the study results give drainage engineers valuable insight to advance their understanding of flow conditions occurring for grade deviations and provide information for consideration in preparing drain installation specifications.

TEST FACILITY

A 17.7-m (58-ft) length of corrugated plastic drain tubing was installed on a tilting flume, where the tubing slope could be changed by raising or lowering the flume, figure 2. The 100-mm (4-in) nominal diameter tubing was nonperforated, and was translucent to allow observations of water and sediment inside the tubing. Lidco Inc., Brawley, Calif., manufactured the tubing.

Test discharges were measured using a stopwatch and a 25-mm (1-in) disk-type watermeter that previously had been volumetrically calibrated. The water was pumped into the head box, stilled when passing through a rock baffle, and then entered the tubing through an elliptical transition, figure 3. A gate in the tail box controlled water surface elevations in the tubing.

The hydraulic gradeline was measured with static head probes placed within the tube as shown in figures 3 and 4. These probes were hydraulically connected to a manometer board with flexible tubing. Markings on the manometer board were in hundredths of a foot and readings were estimated and recorded to the nearest thousandths of a foot. A wetting agent solution was placed inside the manometer tubes to reduce capillary rise. Also, through valving and a manifold, the probes were hydraulically connected to an electrical pressure transducer; and for hydraulic gradelines with small gradients, the pressure could be measured electronically.

Tubing corrugation dimensions are given in figure 5a. These measurements were made on a short, typical segment of tube cut from an 18-m (60-ft) length and do not necessarily reflect dimensional variations along the tube. The inside diameter of 105 mm (4-1/8 in) (fig. 5b) was measured from the inner corrugations. This 105-mm-diameter value was used for *D*, *A*, and *R* in equations (1), (2), (3), and (5), in the section on "Straight Tube Tests." Using outside calipers, measurements were made of the outside tube diameter at locations where the static head probes were installed and are tabulated in figure 5. The distances from the top outside of the tube to the inside invert (D_I) were used for determining invert elevations.

Humps and sags of the vertical bends were formed at a test bend section in the middle part of the 17.7-m (58-ft) long tubing (fig. 3). The bends were 2.4 m (8 ft) long, including transitions necessary to obtain one- and two-diameter (outside-diameter) offsets from grade (fig. 6). Precise curve shapes were made with plywood templates and, when placed in the test section, formed repeatable and accurate bend shapes throughout the studies.

STRAIGHT TUBE TESTS

Full-tube Flow

Two sets of full-tube flow tests were made, one at the beginning of the investigation and the other after the bend tests. In starting the test, the tailwater elevation was set above the top of the tubing and a maximum discharge of 5.7 L/s (0.2 ft^3/s) was established. Even with the maximum discharge, some air remained entrapped in corrugations at the top of the tube. The bubble lengths ranged from 30 to 45 mm (0.10 to 0.15 ft) in a horizontal direction normal

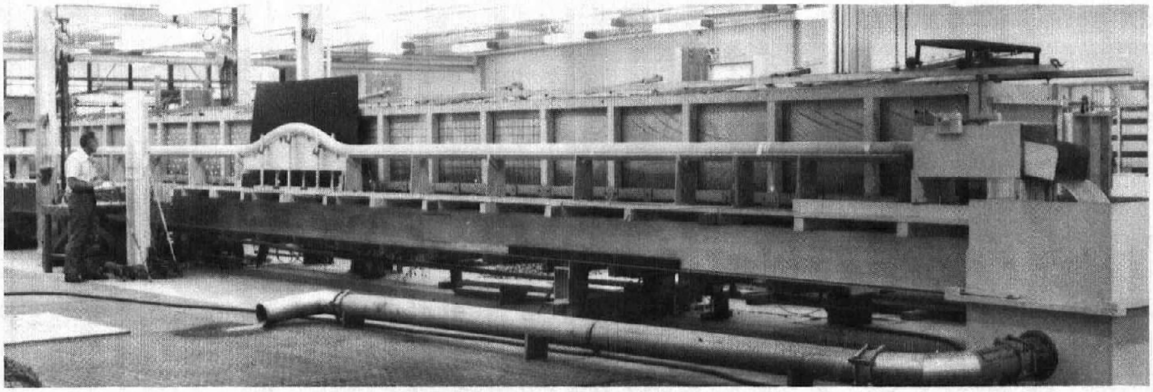

Figure 2.–The corrugated plastic tubing installed on the tilting flume. The test slope *(S)* is approximately 0.01 and the bend with the two diameter offset above grade is in place. Photo P801-D-78805

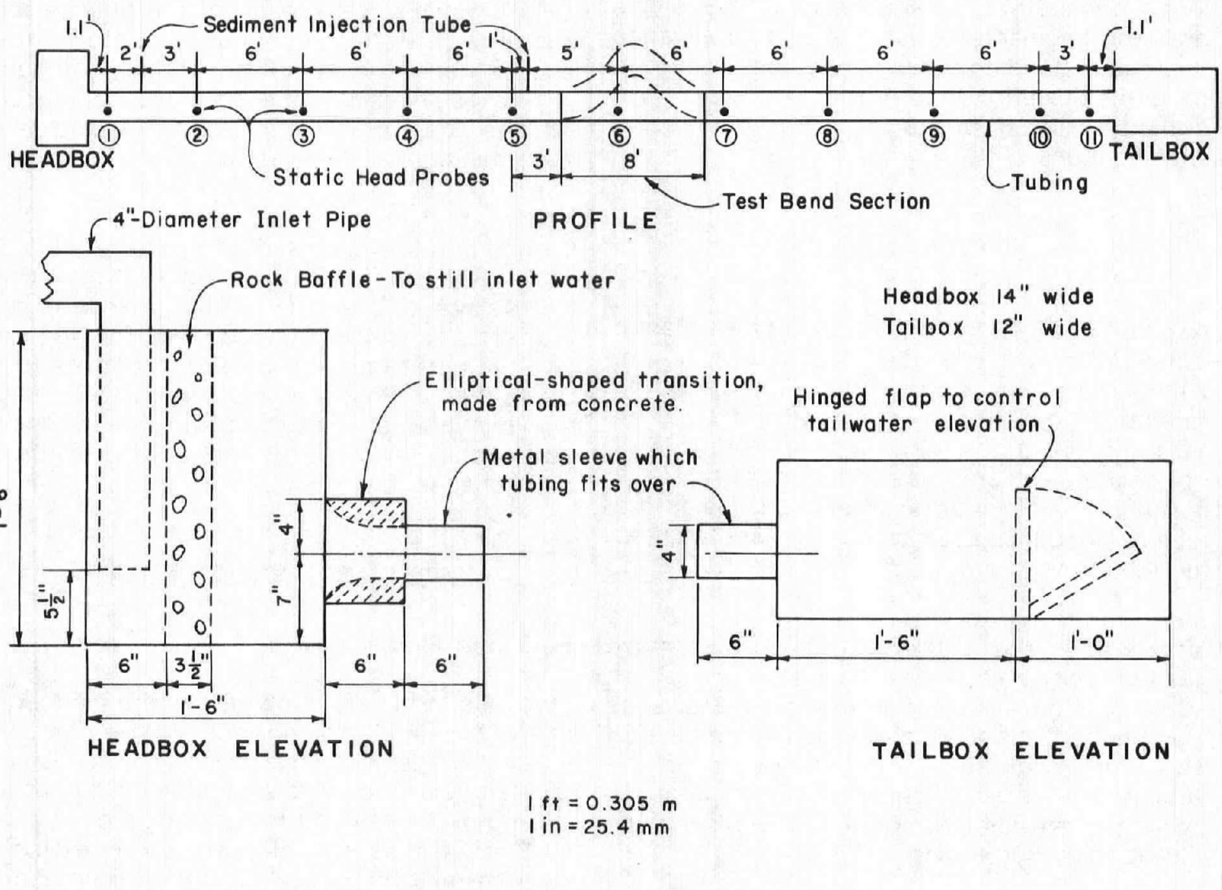

Figure 3.–Test facility.

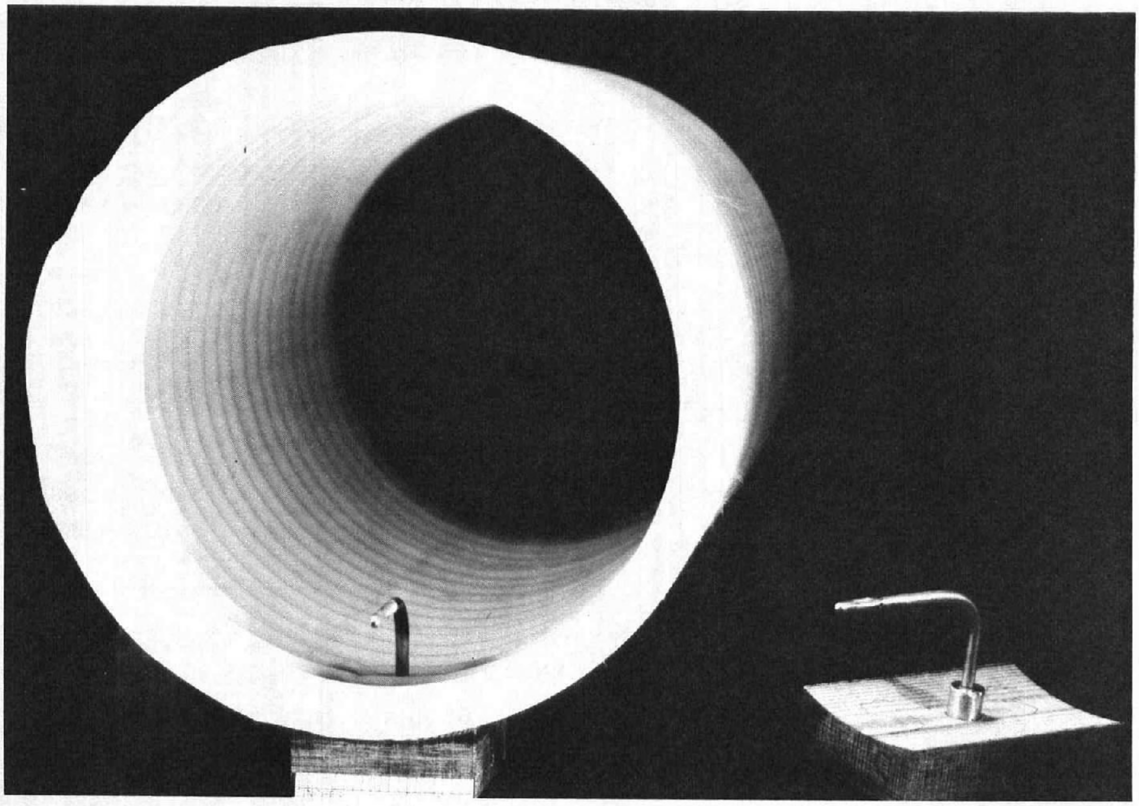

Example of static head probe installation in the corrugated plastic tubing. Photo P801-D-78806

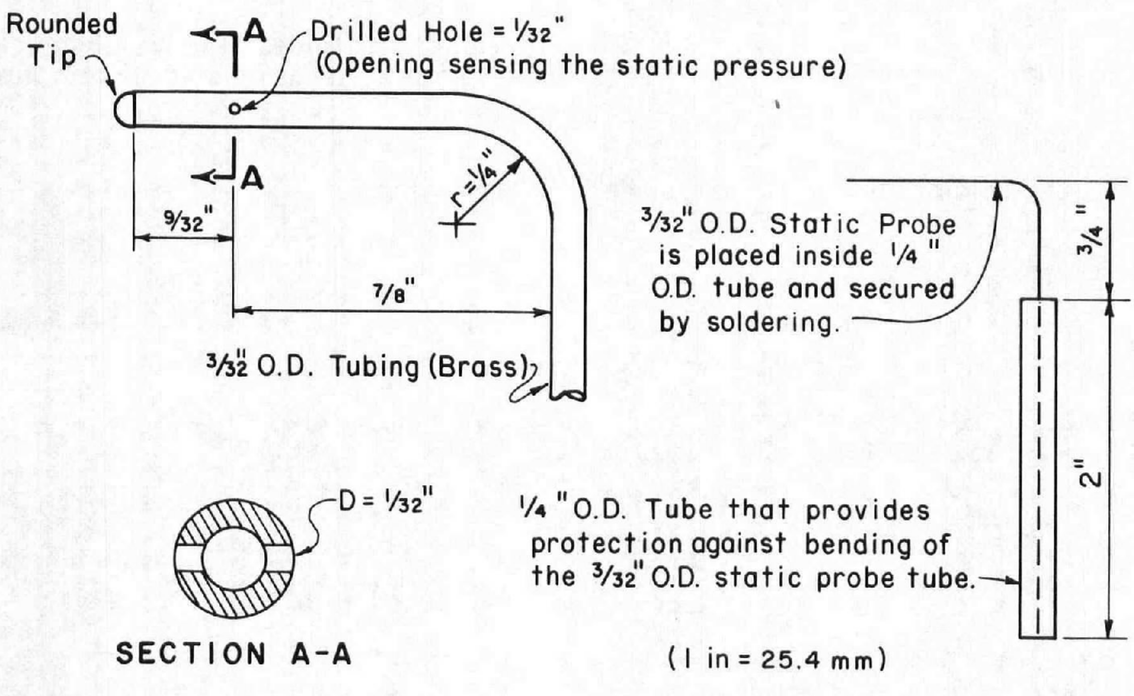

Figure 4.–Static head probes.

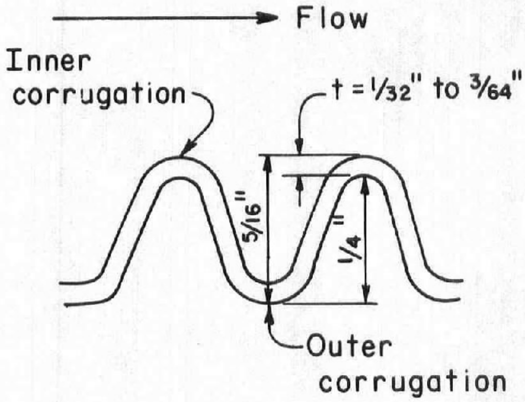

A. Corrugation dimensions

Table A - Outside diameter measurement at the static head probe locations

PROBE LOCATION	D_H INCHES	D_V INCHES	D_V FEET	D_I FEET
1	4.72	4.71	0.392	0.366
2	4.68	4.73	0.394	0.368
3	4.71	4.72	0.393	0.367
4	4.68	4.74	0.395	0.369
5	4.69	4.70	0.392	0.366
6	4.66	4.69	0.391	0.365
7	4.70	4.70	0.392	0.366
8	4.71	4.67	0.389	0.363
9	4.72	4.71	0.392	0.366
10	4.69	4.69	0.391	0.365
11	4.70	4.67	0.389	0.363

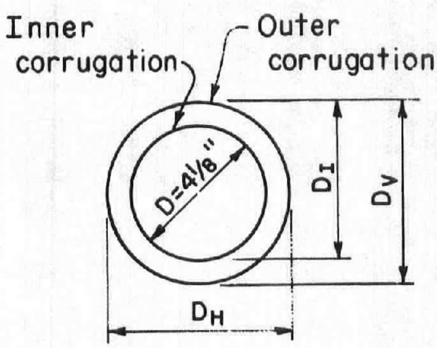

D - Diameter between the inner corrugations 0.344 ft

D_H - Outside horizontal diameter

D_V - Outside vertical diameter

D_I - Distance from top of the tube to the invert, $D_I = D_V - 5/16''$

1 in = 25.4 mm, 1 ft = 0.305 m

The D_I values of table A were substracted from top tube elevations to obtain invert elevations of table 2.

B. Definition of tube diameter dimensions

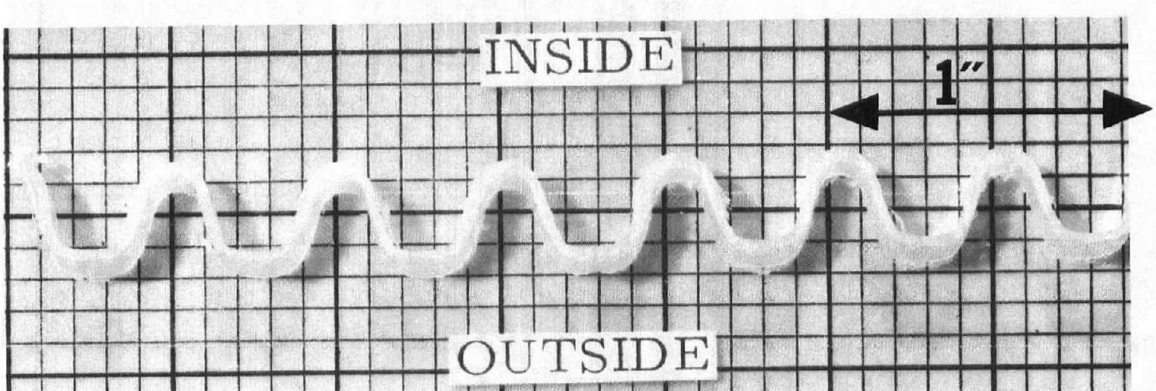

C. Longitudinal section of the corrugated plastic tubing. Inside is the surface boundary for the flowing water.

Figure 5.–Tubing dimensions. Photo P801-D-78807

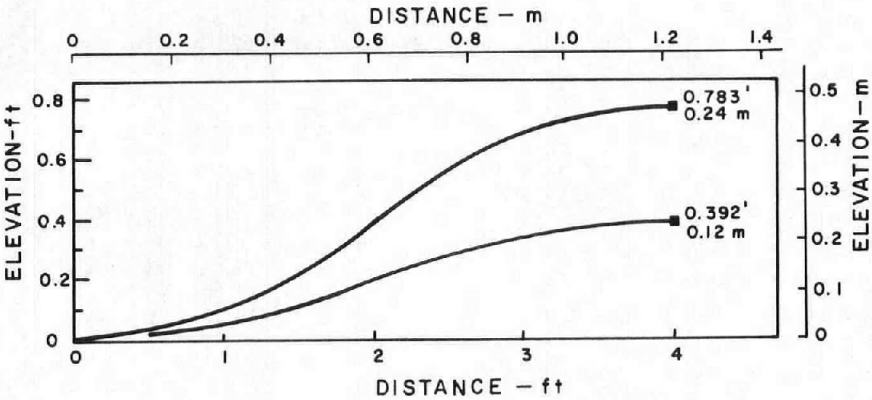

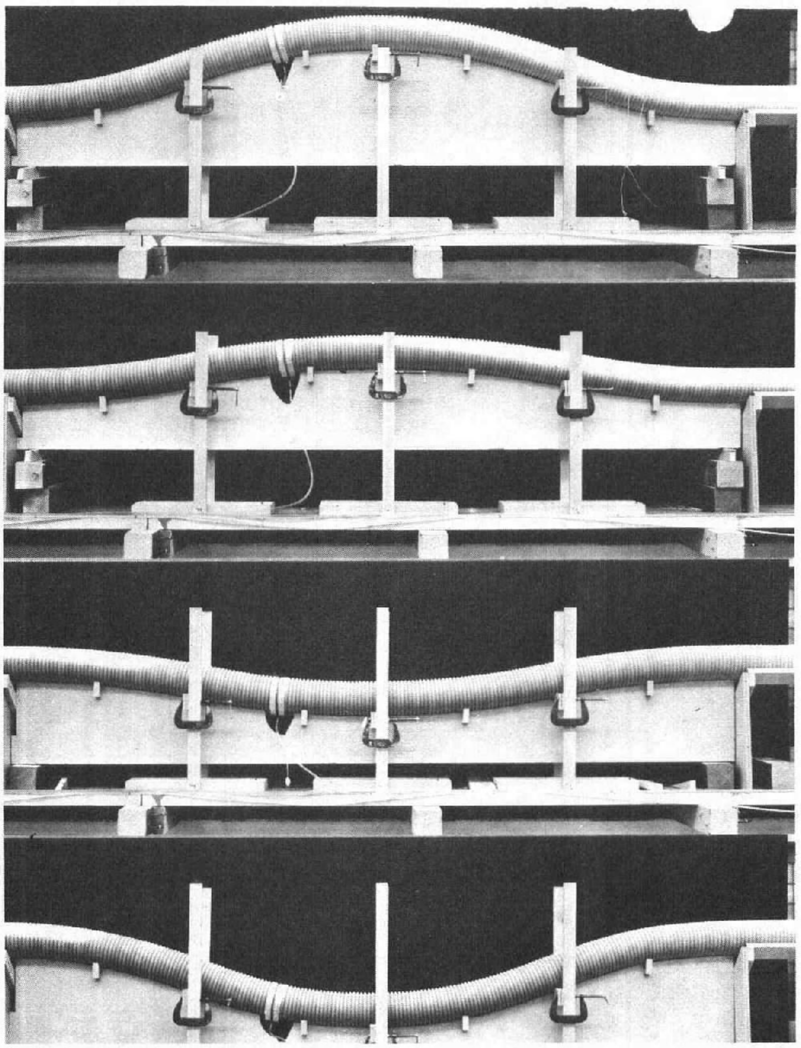

Four test bends–from top to bottom two diameters above, one diameter above, one diameter below, and two diameters below offset from grade. Nomenclature designation of the bends is 2DA, 1DA, 1DB, and 2DB. Test conditions of the photographs are $S \approx 0.02$, $Q = 0.2$ ft³/s, and three-fourths flow depth. Flow is from left to right.

Figure 6.–The four test bends. Photo P801-D-78808

to the tubing centerline. Hydraulic measurements were then made at the maximum discharge and at progressively smaller discharges.

The data collected were discharge *(Q)* and manometer board readings from the static head probes. Readings from probes No. 2 through 10 were used for obtaining the hydraulic grade *(S)*, and a straight-line least squares fit was made to determine a numerical value for the slope. Equations (1) through (5) were used to compute Manning's *n*, Darcy-Weisbach *f*, and the Reynolds number (N_R).

$$V = Q/A \qquad (1)$$

$$V = \frac{1}{n} R^{2/3} S^{1/2} \qquad (2)\ \text{[SI metric]}$$

$$V = \frac{1.49}{n} R^{2/3} S^{1/2} \qquad (2)\ \text{[Customary]}$$

$$\Delta H = f \frac{L}{D} \frac{V^2}{2g} \qquad (3)$$

$$S = \frac{\Delta H}{L} \qquad (4)$$

$$N_R = \frac{VD}{\nu} \qquad (5)$$

where:

Q = discharge (m³/s)
V = average velocity (m/s)
A = flow area (m²)
n = Manning's roughness coefficient
R = hydraulic radius, flow area divided by wetted perimeter (m)
S = slope or hydraulic grade (dimensionless)
ΔH = headloss in meters of water (m)
L = length of tube over which headloss occurs (m)
D = tube diameter (m)
g = gravitational acceleration (m/s²)
N_R = Reynolds number
ν = kinematic viscosity (m²/s)

For free-surface tube flow, equations (3) and (5) may be changed to:

$$f = \frac{8gRS}{V^2} \qquad (6)$$

$$N_R = \frac{VR}{\nu} \qquad (7)$$

Results of the full-tube flow tests are summarized in the plot of Darcy-Weisbach *f* versus Reynolds number (fig. 7); the supporting numerical data are presented in table 1.[1] There is a small decrease in the measured resistance coefficient between the first and second sets of data. This difference was attributed to the measurement variances in repeating the tests.

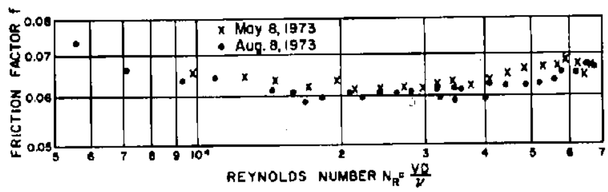

Figure 7.–Friction factor for full-tube flow.

The boundary resistance to water flowing over a rough surface is a function of velocity and is composed of shear and form losses. The tube corrugations form half-circular cylinders, one after another, having wakes and possibly causing a resistance change which varies with velocity. A plot of *n* versus *V* (fig. 8) shows a small variation of *n* between 0.015 to 0.016.

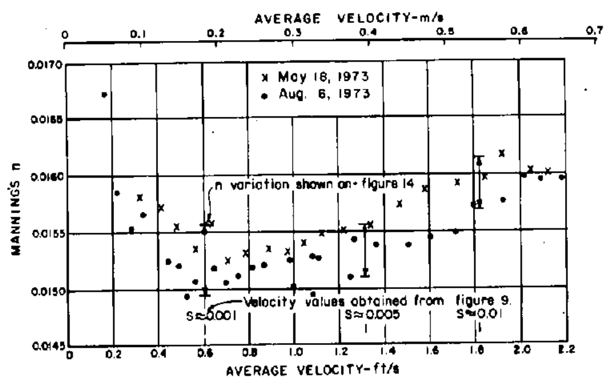

Figure 8.–Manning's *n* versus average velocity for full-tube flow.

---

[1] All numbered tables are contained in appendix 1.

A plot of average velocity versus slope (fig. 9) was used for relating data among tests (fig. 8, 12, 13, and 14).

Free-surface Tube Flow

Introduction

Tests were made for free-surface tube flow with slopes of 0.001, 0.005, and 0.02.

Method of Performing the Tests

Establishing the invert slope and uniform flow conditions in the tubing was more difficult than anticipated. Initially, elevations at static head probe locations No. 1 and 10 were used in setting the slope, and various two-point combinations of static head probe data were used in computing the hydraulic slope. There was considerable inconsistency in the computed n-values. Further investigation disclosed that a least squares fit of data at static head probes No. 2 through 8 gave a more realistic tube slope, and also hydraulic slopes that resulted in less variation in n-values. Static head probe data near the tube entrance and exit were excluded. This technique provided an averaging or a smoothing out of inconsistencies resulting from tube waviness and data measurement variations. From this experience, the following method was developed and used for all tests.

Survey levels were made to determine invert elevations of the tubing. A steel scale marked in hundredths of an inch was used first as a level rod. Later, a point gage reading in thousandths of a foot was used. The point gage had the advantage of a vernier scale that could be used as a target. For each test slope, the elevation of the top of the tubing was determined at the static head probe locations. A vertical distance (D_l, table A of fig. 5) was subtracted from this elevation to establish the tubing invert elevation at the probe locations. Because of the tubing waviness, there were deviations of the invert elevation from a straight line. A least squares fit was made of invert elevations for static probe locations No. 2 through 8 to determine test slopes of the tubing, figure 10. Invert elevations and the tubing slope obtained for the various test slopes are given in table. 2 of appendix 1.

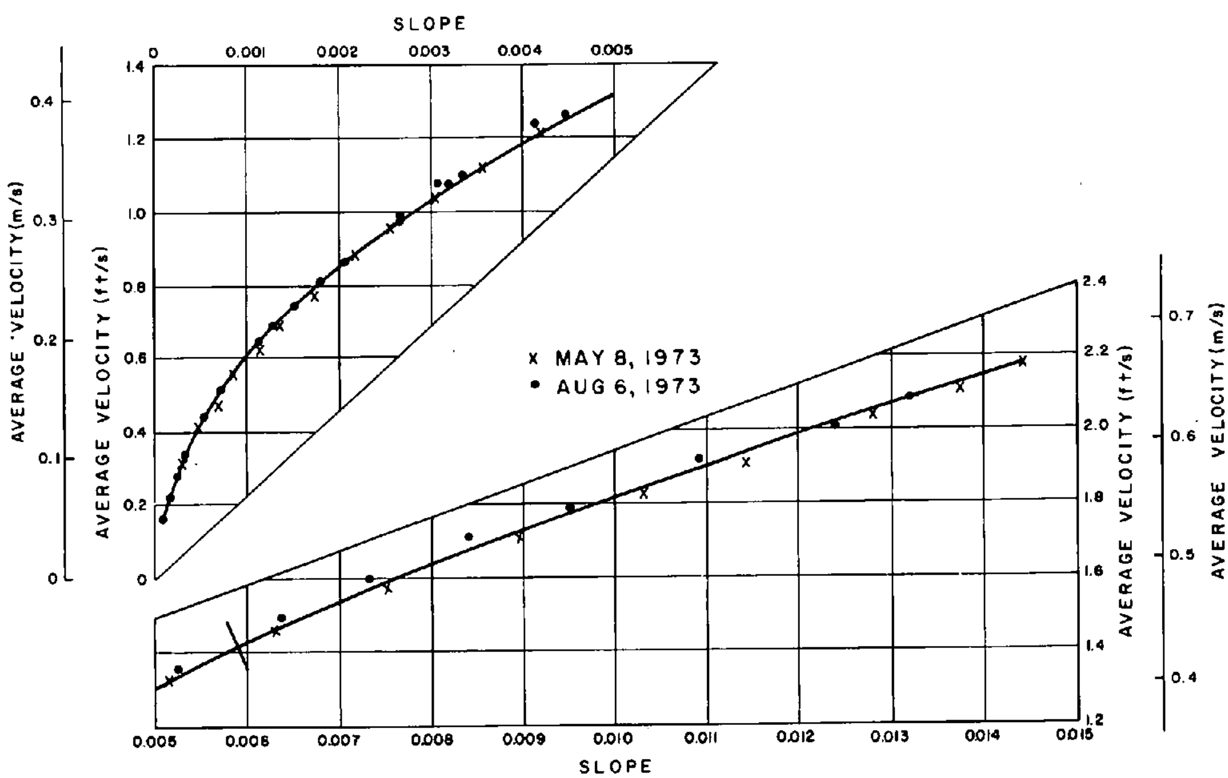

Figure 9.–Velocity versus slope for full-tube flow.

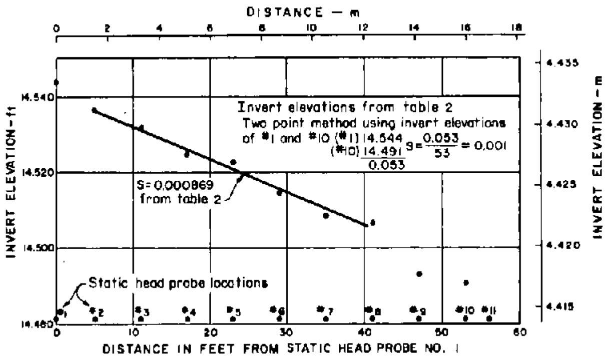

Figure 10.–Comparison of test slopes obtained by two-point method and least squares fit.

Water depths within the tube were measured with static head probes and water manometers. The invert elevations of the tube at the probe locations were referenced to the corresponding manometer, table 2. To determine the water depth at a static probe, the invert reference was subtracted from the manometer reading (fig. 11).

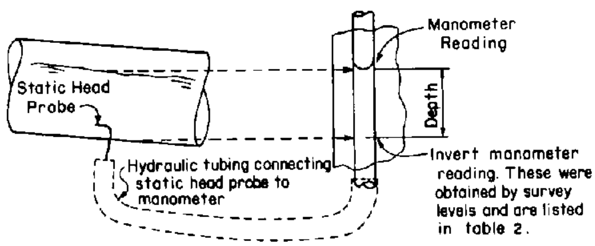

Figure 11.–Schematic showing relation of manometer reading to water depth.

For a given test slope, discharges were varied between about one-fourth flow depth and slightly less than full-tube flow. Difficulty was encountered in establishing uniform flow in the tube. For each discharge, adjustments were made to the tailwater control gate (fig. 3) in an effort to get a uniform flow depth. Preliminary observations of manometer readings and computations for flow depth were made at the static head probe locations. If flow depths were not similar along the static head probe locations, then further adjustments were made to the tailwater control gate. When water depths appeared uniform, the manometer readings were recorded.

Test Results

The difficulty of deciding whether uniform flow was established is illustrated by the inconsistent water depths along the tubing; see table 3. To show variation of the test results, the individual water depths were used to compute the flow areas. Then velocity, Manning's *n*, Reynolds number, and friction factors were computed with equations (1) through (7), using the least squares hydraulic slope. Had individual hydraulic slopes between probes No. 2 and 3, 3 and 4, etc., been used in the computations, there would be greater variance in the test results.

The water depth variance was resolved by using the average water depth for computing the flow area. The test results are shown at the bottom of table 3.

Numerical results of all tests are given in table 4. A graph of water depth versus average velocity is shown in figure 12, water depth versus discharge in figure 13, and water depth versus Manning's *n* in figures 14a through 14d. In the figures, the water depth is designated uniform depth because of the uniform flow in the tubing.

Difficulty was encountered in establishing test conditions when the tube was nearly full. Slight increases in the test discharge and control gate elevation readily changed the flow from free-surface to full-tube flow. With full-tube flow, a slight decrease of tailwater elevation allowed the water to separate from the tube roof. The separation point progressed upstream and free-surface flow occurred in a downstream part of the tubing and full-tube flow in an upstream part. Measurements were not made for flows in this transition range. However, data from full-tube flow were used to indicate limits in this range. Full-tube flow velocities were obtained for test slopes 0.001, 0.005, and 0.01 from figure 9 and were plotted on figure 12. These velocities were multiplied by the full-tube flow area to obtain the discharges of figure 13.

In figures 12 and 13, the maximum average velocity and discharge occur between 76- and 92-mm (0.25- and 0.30-ft) depth and then decrease as the flow changes to full-tube flow. The computed Manning's *n* varied with flow depth (figs. 14a, 14d, and 15). At small depths, the Manning's *n* was near maximum at 0.018, approached a minimum near the one-half flow depth, and increased to another maximum near full-tube flow depth. The lines shown on figure 14 and repeated in figure 15 were drawn by inspection.

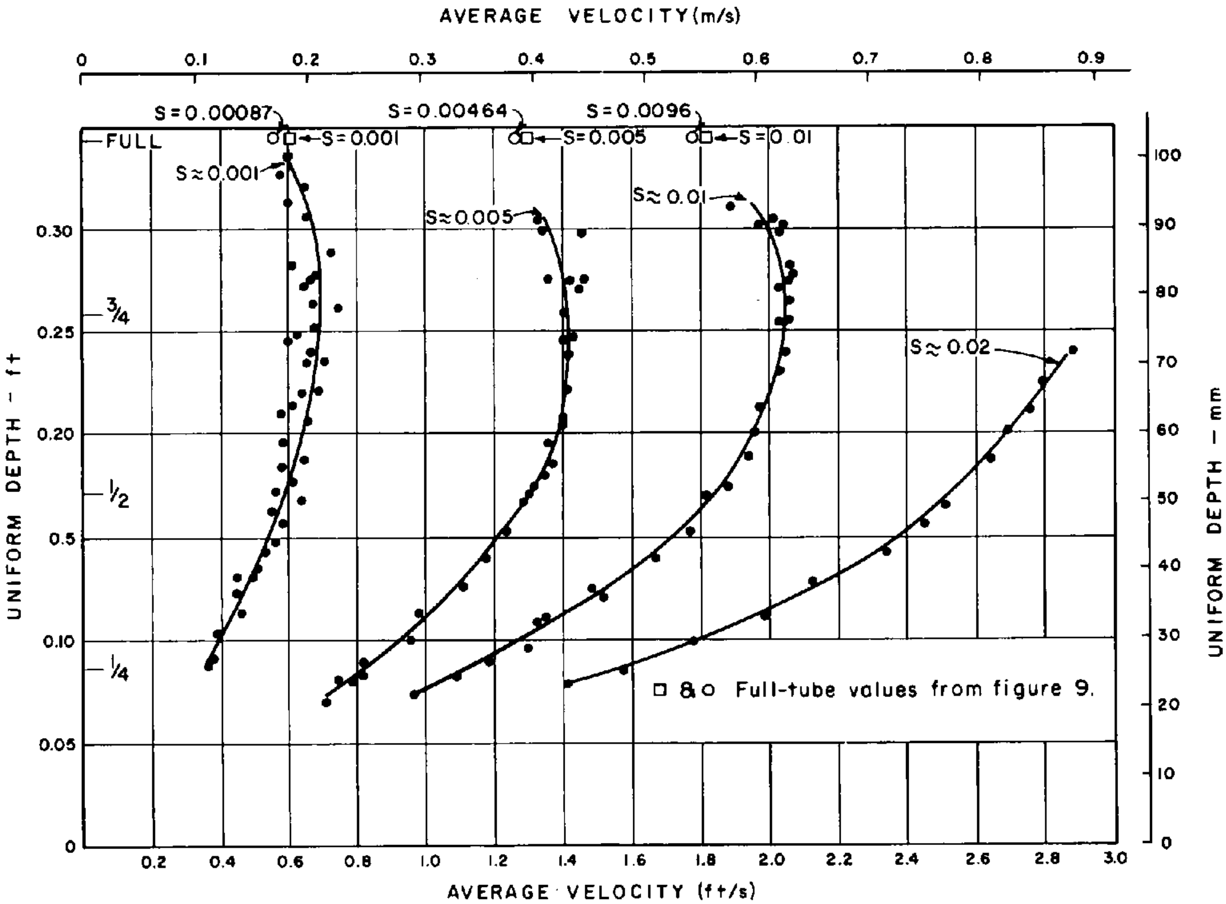

Figure 12.–Uniform depth versus average velocity.

BEND TESTS

Introduction

The limited length of the test facility precluded using gradual grade deviations that typically could occur in field installation. However, short length or small radius bends were expected to provide more resistance to flow than long ones and were believed adequate to show hydraulic consequences of significant grade deviations. The length of the bends, including transitions, were 2.4 m (8 ft), and the outside tube diameter was used as the vertical offset distance. For a given bend the curve was marked on a sheet of plywood and then cut to form a curve template that was used as the tube support. The bends were designated 2DA, 1DA, 1DB, and 2DB; that is, two and one diameters above grade, and one and two diameters below grade.

The bend tests were initially made with one-fourth, one-half, three-fourths, and full-tube flow depths at several tube slopes. Later, several tests were made at other depths.

Constant-flow Depth Tests

The discharges to produce the required one-fourth, one-half, and three-fourths flow depths were obtained from figure 13. These were set and adjustments were made to the tailwater elevation to establish a uniform water slope within the straight tube. Measurements of the hydraulic gradeline were then made. While the water was flowing at a constant rate, each bend was placed successively in the test section, measurements were made, and the test series was concluded by returning to the straight tube condition. Tests were made at slopes of 0.001, 0.005, and 0.02, and the results are presented

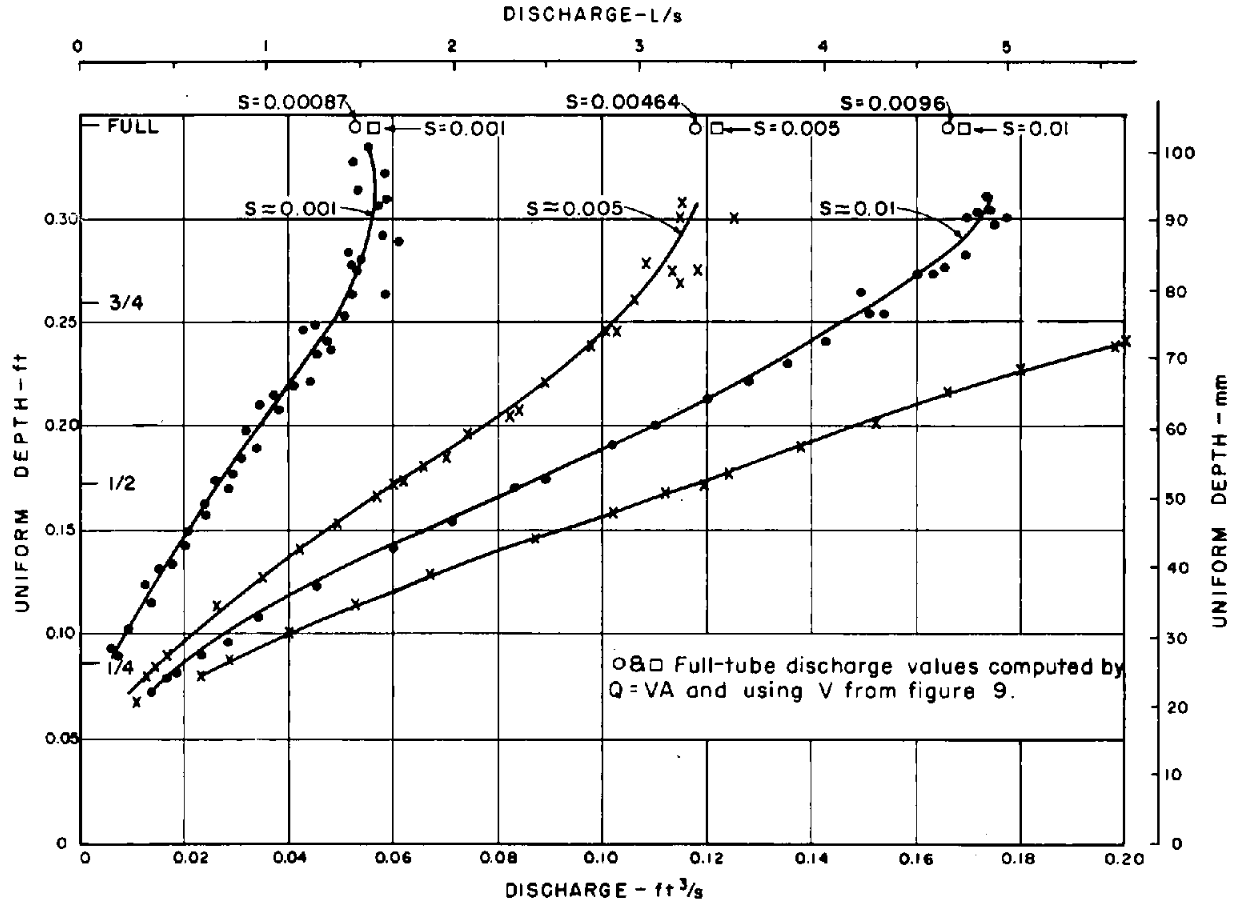

Figure 13.-Uniform depth versus discharge.

as graphs of the hydraulic gradelines (figs. 17, 18, and 19). To show differences in the hydraulic gradelines, the ordinate scale was expanded. This caused an extreme distortion of the bend shape and prevented showing the shape on the figures. Therefore, the bend flow surfaces were omitted between the 26- and 34-ft marks of the abscissa scale. Interpreting the graph requires the reader to visualize the bend in place similar to that shown in figure 16.

Results for the 0.001 test slope are shown in figure 17. The ordinate scale is that of the manometer board in feet of water and the abscissa scale is distance in feet along the tube. Top and bottom flow surfaces of the tubing are shown with wide lines and are located at the inner corrugation of the tubing (fig. 5b). The tube invert was drawn through elevation points (obtained from table 2) and the top tube flow surface was drawn a vertical distance of 105 mm (0.344 ft) above the bottom.

Hydraulic gradelines for the straight tube are those shown within the wider lines. After placing bends of one- and two-diameter offsets above grade in the test section, the hydraulic gradelines rose accordingly and full-tube flow occurred upstream from the bends. These upstream gradelines are designated data 1DA and data 2DA on figure 17. Flow passing over the bend crests and into the downstream straight tube occurred with a free surface and the downstream hydraulic gradelines coincided with those of the straight tube. For bends below grade, the upstream and downstream hydraulic gradelines coincided with those of the straight tube. This coincidence can be seen in table 5 and by comparing manometer readings of the 1DB and 2DB tests to the straight tube test.

Figure 20 shows photographs of water surface profile variations through the bends for the test series with a 0.001 slope. The water was dyed red so it would show through the translucent

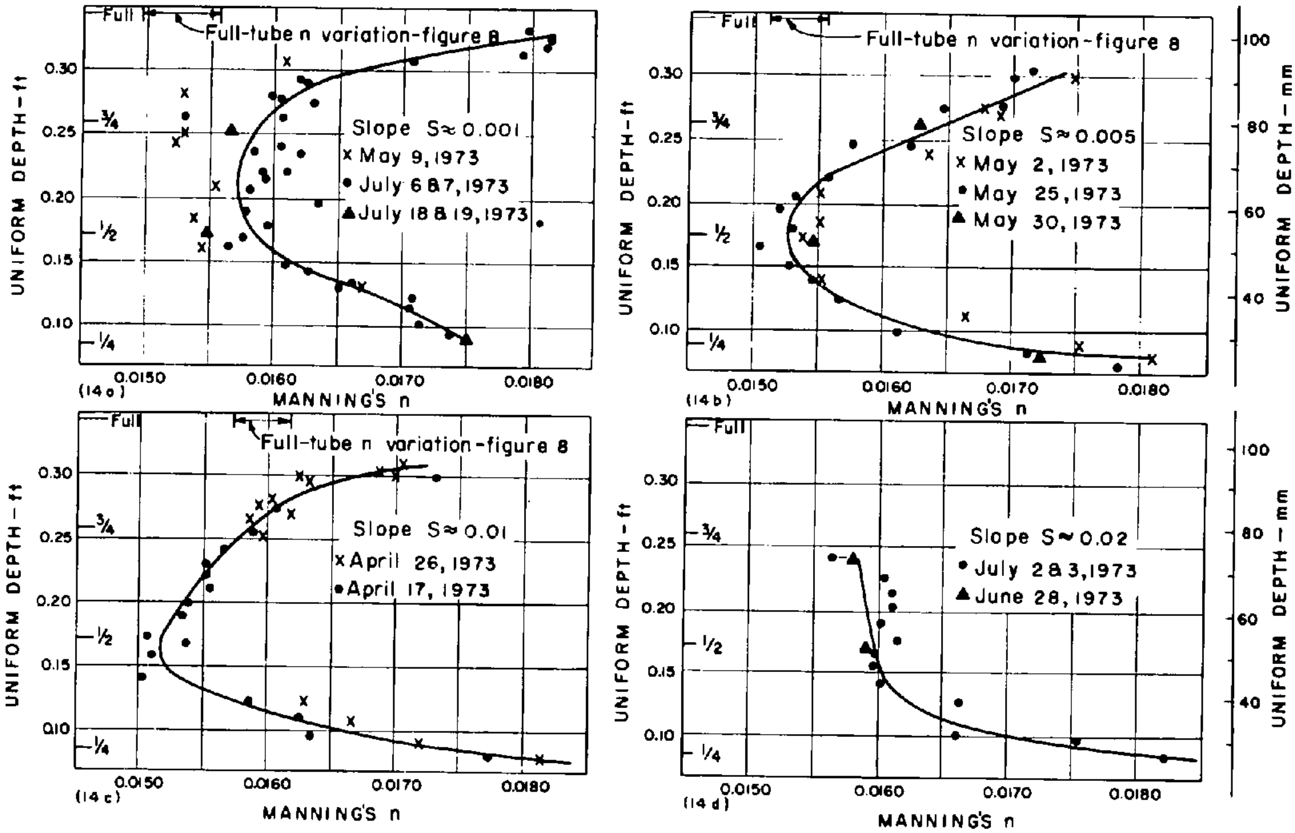

Figure 14.–Uniform depth versus Manning's *n*.

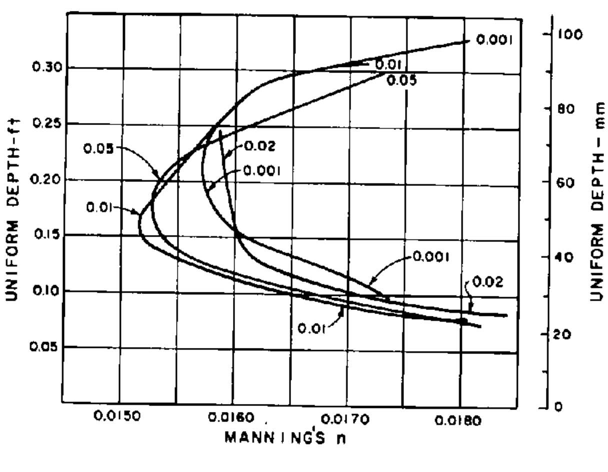

Figure 15.–Uniform depth versus Manning's *n*, comparison for test slopes.

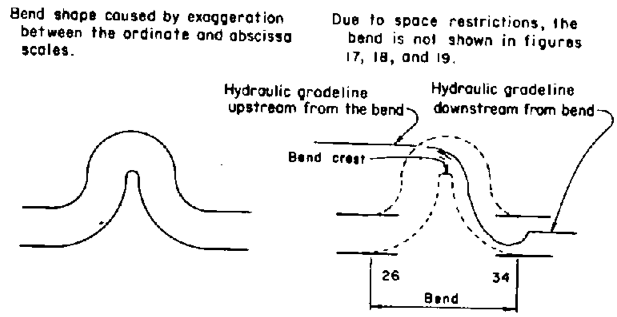

Figure 16.–Schematic showing graphical distortion of bend.

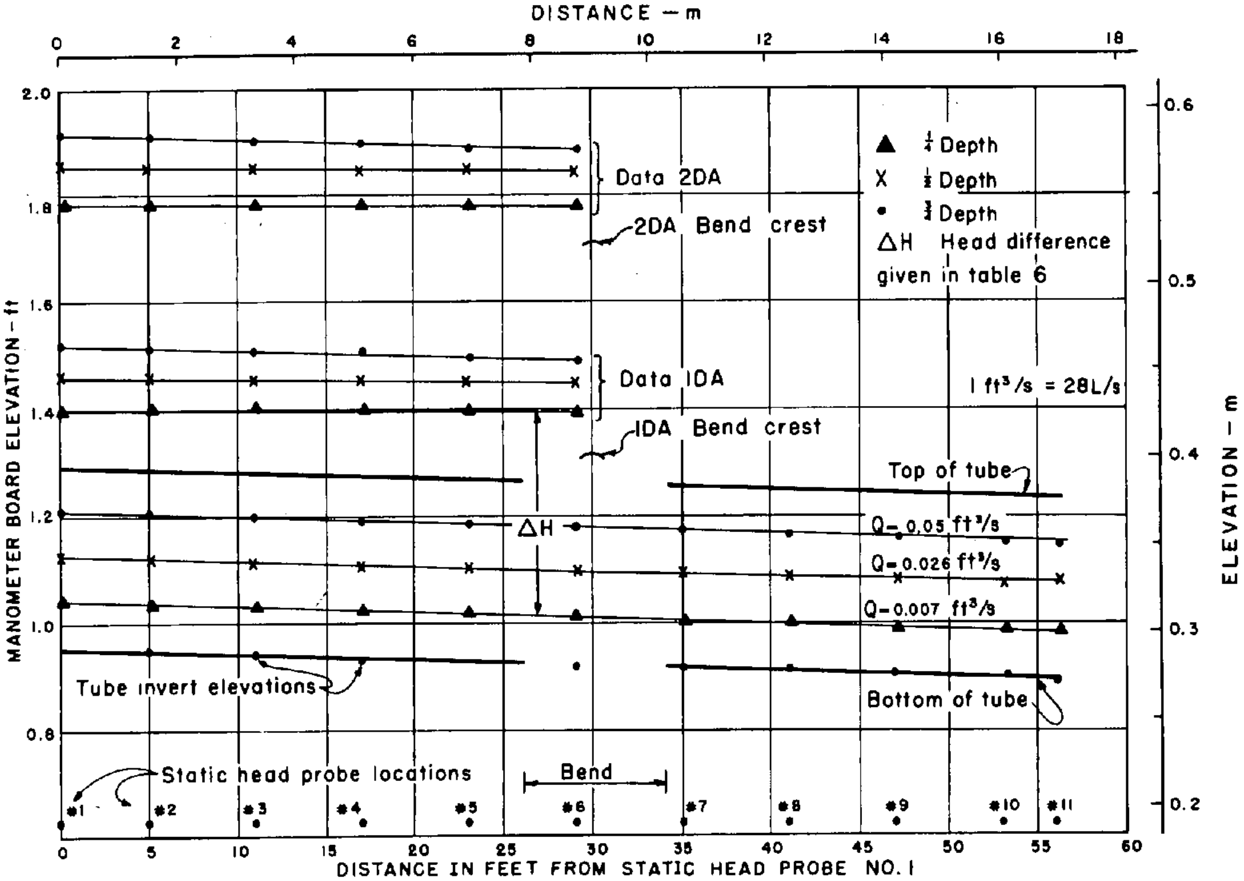

Figure 17.–Hydraulic gradelines for bend tests, $S = 0.001$.

tube. For bends above grade, there was supercritical flow downstream from the crest and a hydraulic jump. As discharges and flow depths increased, the jump moved very slightly upstream. For bends below grade, the bend filled with water and the flow entered and exited from the bend smoothly, similar to an inverted siphon.

For the one-fourth and one-half flow depths at the 0.005 test slope, the tailwater control gate had been adjusted too high and there was a backwater effect at static head probes 9, 10, and 11. The backwater effect did not extend upstream to the bend test section (fig. 18).

Because of the steep 0.020 slope, backwater effects from the 1DA bend at the one-fourth flow depth did not extend upstream to the head box (fig. 19). There was uniform flow from points a to b, then transition to full pipe flow from points b to c, and full pipe flow from points c to d. A hydraulic jump did not form downstream from the 1DA and 2DA bends because the 0.02 slope was evidently supercritical. Downstream from static head probes No. 8 or 9, the supercritical flow returns to uniform flow or the straight tube condition.

For 1DB and 2DB bends and at the three-fourths depth, the upstream hydraulic gradelines were slightly higher than for the straight tube tests (fig. 19). These were the only tests where upstream hydraulic gradelines for bends below grade differed from those of the straight tube. At the upstream leg of the bends, there appeared to be a closed conduit hydraulic jump (lower two photographs of fig. 6) that provided resistance, and this resistance apparently raised the hydraulic gradelines.

For the constant-flow depth tests, bends below grade had a negligible effect on the hydraulic gradeline, and bends above grade raised the hydraulic gradeline about equal to the offset of

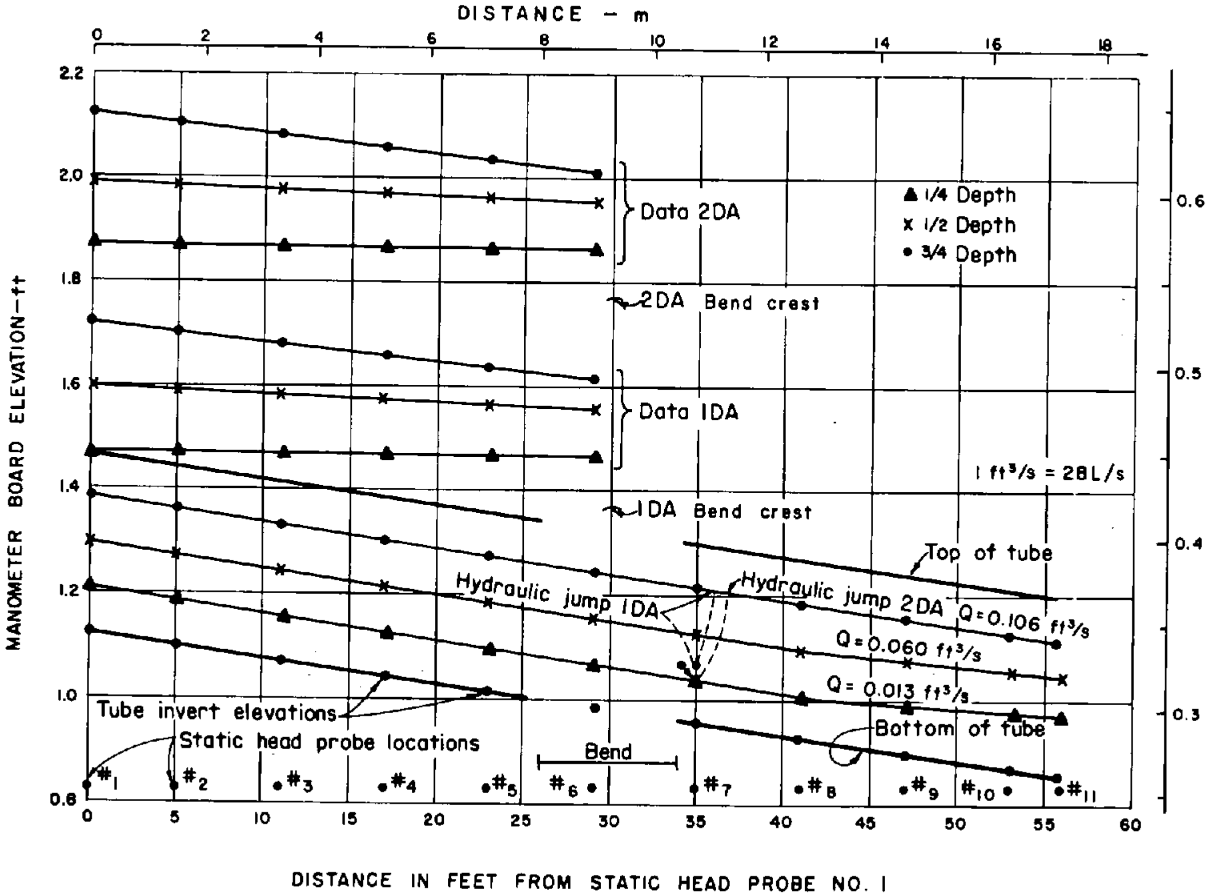

Figure 18.–Hydraulic gradelines for bend tests, $S = 0.005$.

the bend above grade. Head differences between hydraulic gradelines of the straight tube and bend are given in table 6.

Full-tube Flow Bend Losses

Bend loss measurements were made for full-tube flow with the four bends using a 5.49 L/s (0.194 ft³/s) discharge. Without changing the discharge, each of the four bends (2DA, 1DA, 1DB, and 2DB) was formed successively in the test section. The hydraulic gradelines were determined for the straight tube, for each bend, and for the straight tube again after completion of the bend tests. Because of the bend flow resistance, the hydraulic gradelines upstream from the bends were expected to be higher than for the straight tube. However, after placement of the 1DB bend, the upstream gradeline lowered below that for the straight tube. Also, for the straight tube condition, the ending gradeline was 6 mm (0.02 ft) lower than for the beginning gradeline. Therefore, these tests were judged deficient because of the nonrepeatability of the straight tube test condition.

Changes in the number or volume of small air bubbles trapped in corrugations at the top of the tube in the bend section may have contributed to the poor repeatability of the tests. During placement of the 2DA bend, bubbles in the corrugations of the straight tube escaped and collected into a large bubble in the top of the bend. The bubble was 0.23 m (0.75 ft) long and 20 mm (0.07 ft) down from the top inside flow surface of the tube. The bubble changed to 0.43 m (1.4 ft) long and with its surface 15 mm (0.05 ft) below the crown when the 2DA bend was reduced to 1DA. When the 1DB bend was placed in the test section, the large air bubble broke into smaller bubbles which traveled

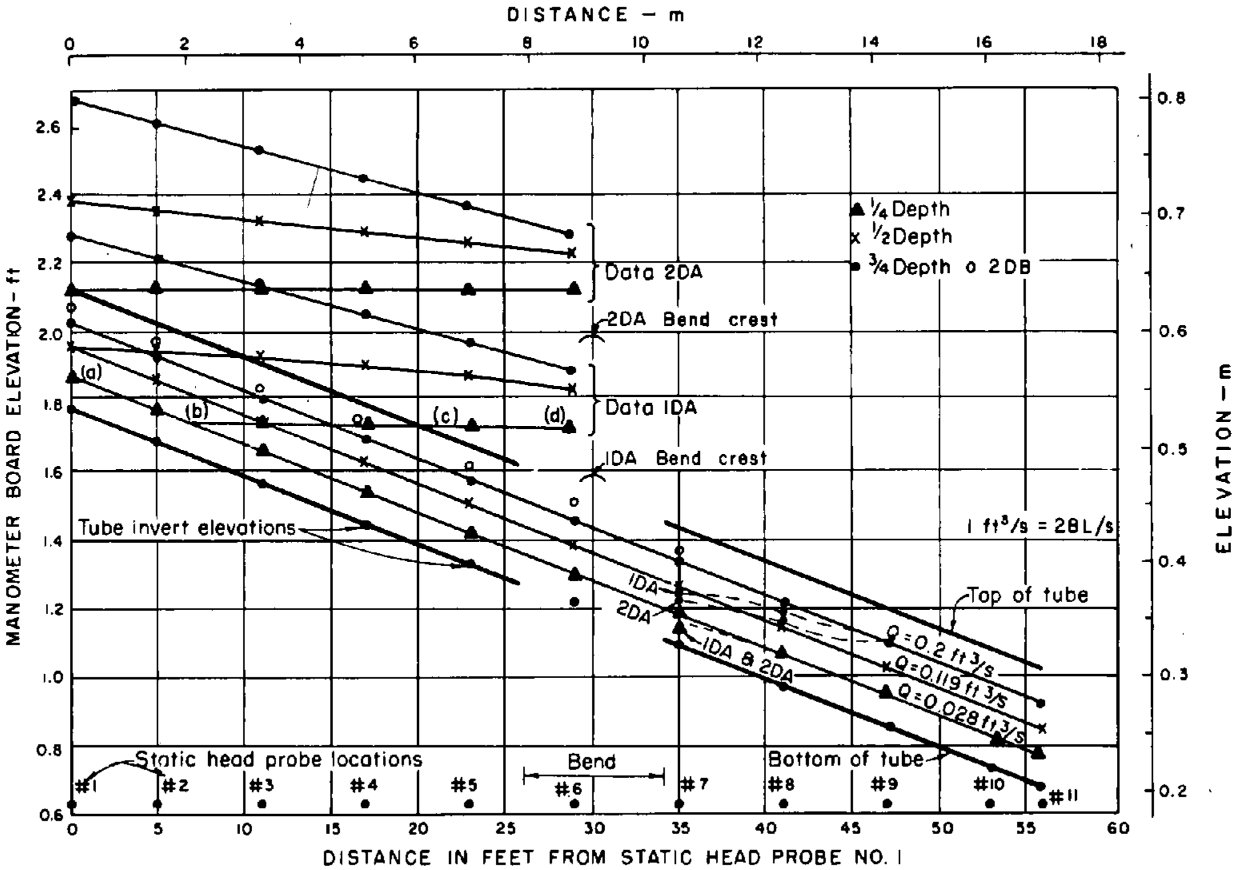

Figure 19.–Hydraulic gradelines for bend tests. $S = 0.020$.

downstream along the top of the tube and out into the tail box. Thus, loss of air in the tube near the test section may have slightly lowered the resistance to waterflow.

In an attempt to obtain repeatability, additional tests were made using only the 2DB bend because a large bubble would not form and be trapped in this bend for full-tube flow conditions. Three test discharges were used and the series was started with the lowest one. Data were taken for the straight tube, then with the 2DB bend, and finally for the straight tube again. The upstream hydraulic gradeline was 3 mm (0.01 ft) higher for the first straight tube test than for the ending one.

While placing and removing the bend, air bubbles were flushed from the test section. With the facility still operating at the low discharge, the tests were done again. Hydraulic gradelines were within 0.6 mm (0.002 ft) for the starting and ending straight tube tests. With continuous operation of the facility, tests were made with the other two discharges. Similar repeatability was attained.

Head differences between bend and straight tube measurements were obtained for static probe locations No. 2, 3, and 4. These three head differences were averaged to get the bend loss for a given discharge. The formula

$$\Delta H = K\frac{V^2}{2g} \tag{8}$$

was used to compute values of the headloss coefficient K for the full-flowing tube:

	First discharge	Second discharge	Third discharge
Test discharge (Q, L/s)	2.62	3.44	4.90
Velocity (V, m/s)	0.305	0.399	0.567
Bend loss (ΔH, mm)	2	4	9
Bend loss coefficient (K)	0.45	0.53	0.56

Other Flow Depth Tests

Tests were made for the 2DA and 2DB bends at a tube slope of 0.005, with variable discharges which produced flow depths other than one-fourth, one-half, and three-fourths. Discharges were progressively increased and eventually increased to full capacity in each test series for each bend. The intent was to simulate a field condition of increasing drain discharge as summer irrigation progressed.

Hydraulic gradelines for some of the 2DA bend test discharges are shown in figure 21. The hydraulic gradelines are identified by test number with corresponding test discharges. Water surface profiles with air trapped in the bend are shown in figure 22.

Uniform depth for the test discharges was obtained from figure 13 and set at static head probe No. 8 with the tailwater control gate. At a discharge of 3.28 L/s (0.116 ft^3/s), the hydraulic jump downstream from the bend contacted the top of the tube, and for all higher discharges no further adjustments were made to the tailwater control gate. The tube was allowed to control gradient for the larger test discharges and a longer operation time was required before taking data.

Hydraulic gradeline elevations, both upstream and downstream from the bend, progressively increased as the discharge increased from 0.37 to 3.14 L/s (0.013 to 0.111 ft^3/s), figure 21. Near full-tube flow at a 3.28-L/s (0.116-ft^3/s) discharge, the hydraulic jump contacted the tube top 0.46 m (1.5 ft) downstream from the bend. An air cavity was trapped within the bend, figure 22a. Action of the jump tended to pull air bubbles from the cavity, thus reducing the pressure. This caused lowering of the upstream gradeline and was the beginning of siphon-type flow within the bend.

Further increases in discharge increased the siphon-type action and further lowered the upstream hydraulic gradelines. There was an unstable pressure condition upstream from the bend at 3.34 L/s (0.118 ft^3/s), and water level elevations in manometers 1 through 6 raised and lowered over a 4- to 10-min interval. This range of fluctuation is designated by the small vertical rectangles in figure 21. Air bubbles were carried from the air cavity, and the jump moved 0.46 m upstream to the end of the bend. A gentle upstream tube slope at this location was believed conducive to the 90-mm (0.3-ft) up and downstream movement of the jump. As the jump moved, the pressures fluctuated.

To show the siphoning effect, manometer readings of static head probe No. 8 (located downstream from major effects of the hydraulic jump) were subtracted from readings of probe No. 5 (upstream from the bend). This head difference was plotted against discharge, figure 23. Upon approaching the 3.40 L/s (0.12 ft^3/s) full-tube flow condition, the siphoning takes place rapidly with a relatively small increase of discharge. The adjusted head difference curve, table 7 and figure 23, provides a better illustration for bend effect because the equivalent straight tube head loss between probes No. 5 and 8 was considered. This curve shows siphoning gradually improved as discharges were increased beyond 3.40 L/s (0.12 ft^3/s).

Note the relation of air cavity size, shown in figure 22, with respect to the adjusted head difference curve of figure 23. The smaller air cavity is associated with the greater siphon effect through the bend.

Hydraulic gradelines for some of the 2DB bend test discharges are given in figure 24 and water surface profiles in figure 25. For tests with free-flow conditions, the tailwater was adjusted

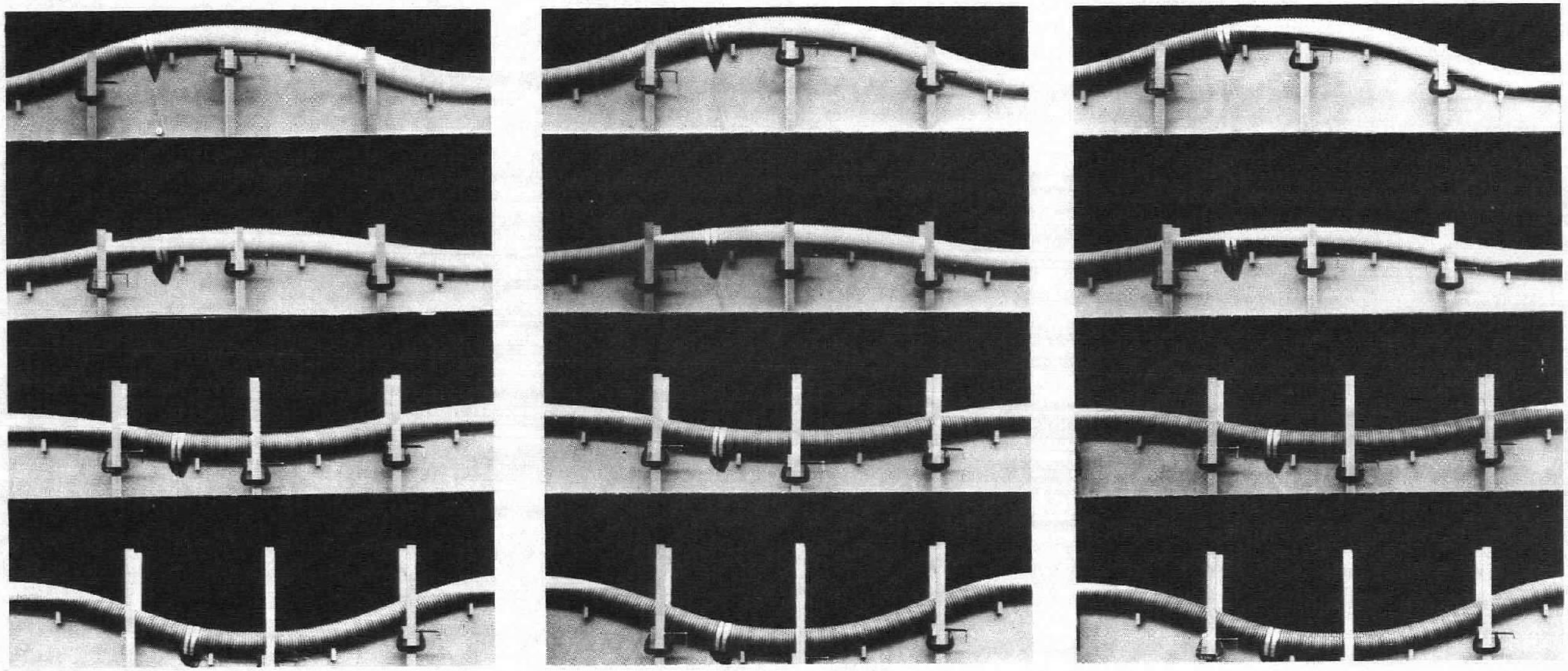

1/4 flow depth 1/2 flow depth 3/4 flow depth

Figure 20.–Photographs showing water surface profiles in the bends, $S = 0.001$. Photo P801-D-78809

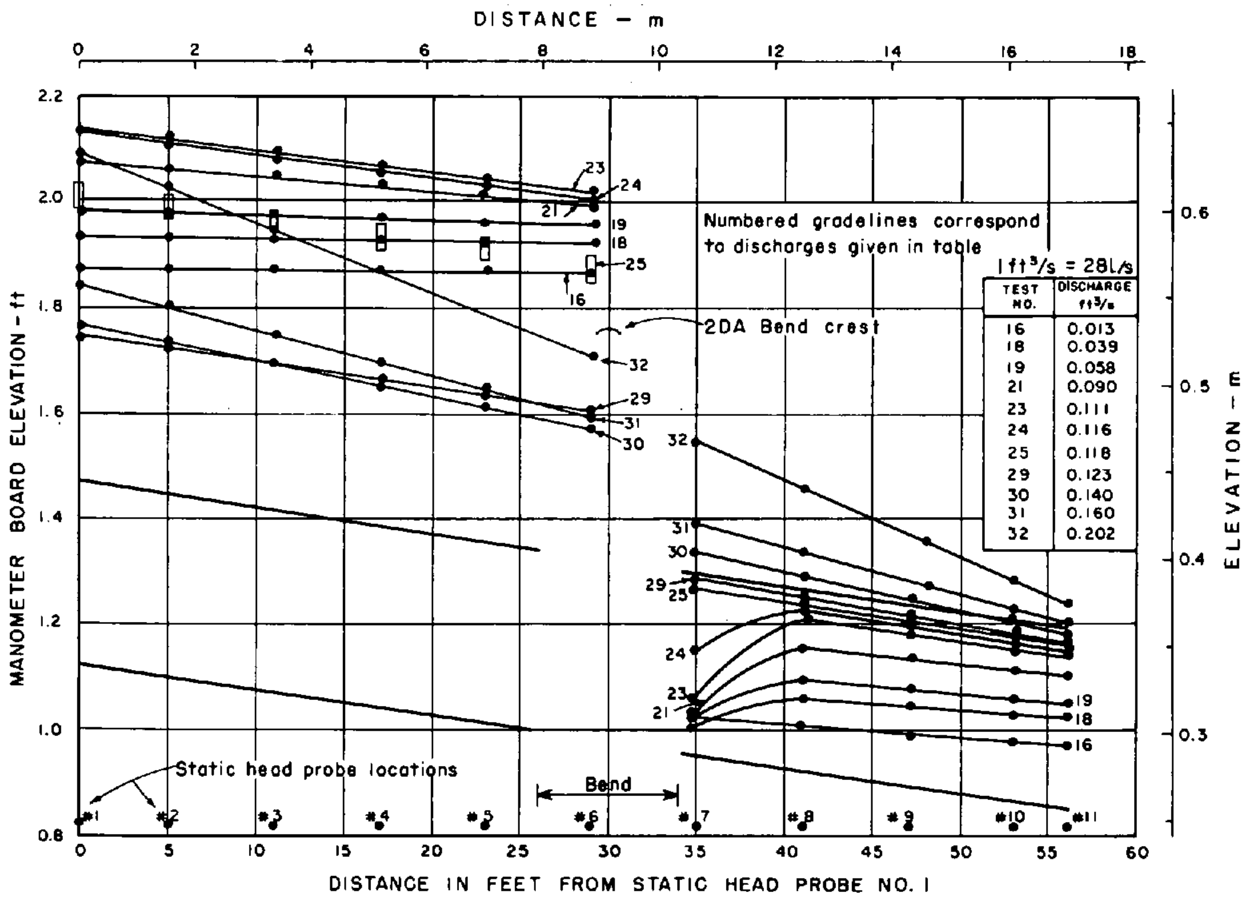

Figure 21.–Hydraulic gradelines for 2DA bend, $S = 0.005$.

to provide uniform flow depths at probe location No. 8. After 3.34 L/s (0.118 ft³/s) discharge, no further adjustments were made to the tailwater box flap because test discharges were greater than the full-tube flow discharge. As test conditions were established for 3.62-L/s (0.128-ft³/s) discharge, the water surface elevation in the head box rose above the top of the tube and air was entrapped in the tube upstream from the bend. The furthest upstream extension of the bubble is designated the contact point and is referenced, in feet, from the tube inlet (fig. 25). At the 4.39-L/s (0.155-ft³/s) discharge, a hydraulic jump formed at the entrance of the 2DB bend. The turbulent action entrained small air bubbles, removed them from the air cavity, and caused the hydraulic gradeline upstream from the bend to lower. Thereafter, the manometer water levels were observed, and if the levels did not lower in a 5-min interval, stable conditions were assumed and then recorded.

Head differences for the 2DB bend tests are shown on figure 23 and in table 7. Shape of the air-water interface has some relation with the adjusted head differences. When hydraulic jump-type flow was present, with accompanying turbulent flow, 4.39 to 5.21 L/s (0.155 to 0.184 ft³/s), the adjusted head differences were greatest (fig. 25). Head differences for the 2DB bend were less than those of the 2DA bend (fig. 23).

The other flow depth test results provide important considerations to the drainage engineer regarding grade specifications for drain construction. The bend below grade had a negligible effect on the hydraulic gradeline. Thus, bends below grade appear nondetrimental for reducing effective drainage depth below ground level for a drain. The bend above grade was detrimental to drainage because the gradeline upstream from the bend was raised

(a)

(b)

(c)

(d)

(e)

(f)

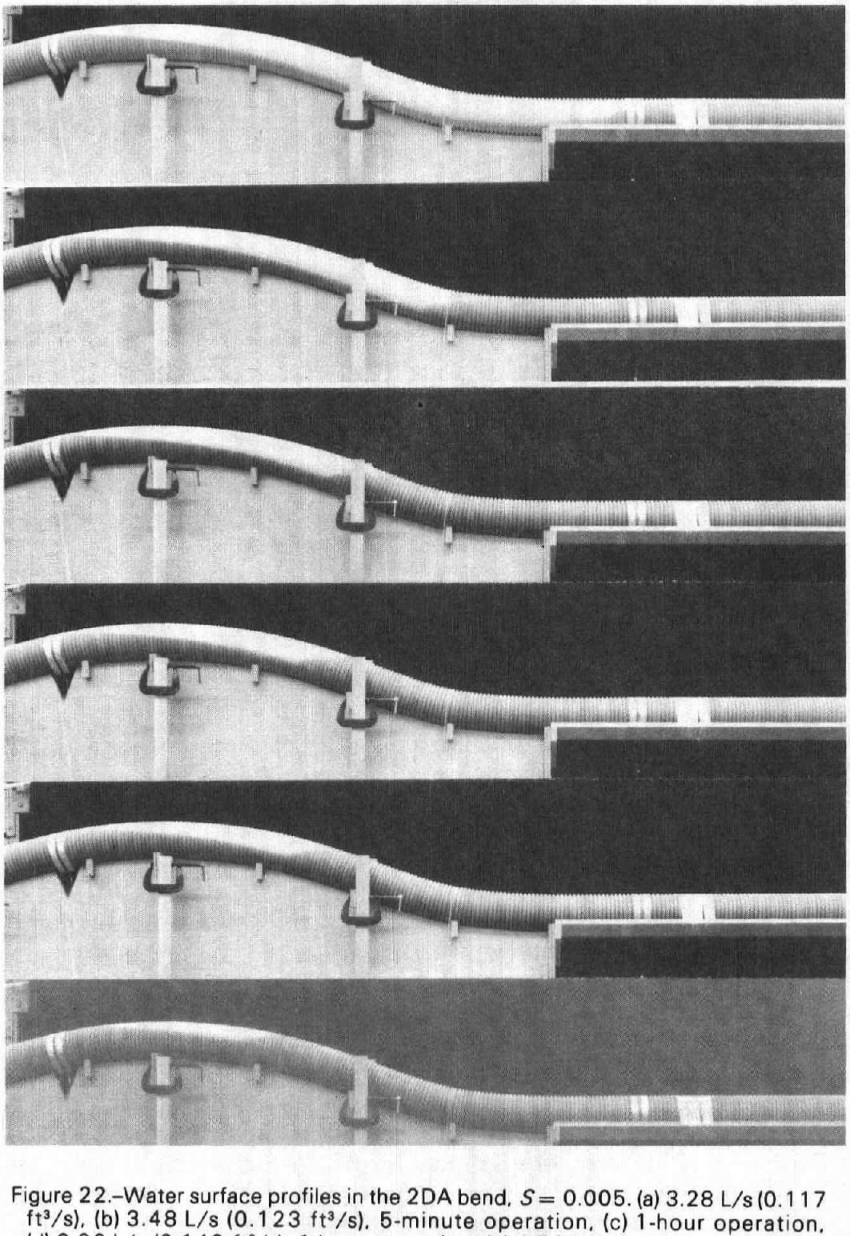

Figure 22.–Water surface profiles in the 2DA bend. $S = 0.005$. (a) 3.28 L/s (0.117 ft³/s), (b) 3.48 L/s (0.123 ft³/s), 5-minute operation, (c) 1-hour operation, (d) 3.96 L/s (0.140 ft³/s), 1-hour operation, (e) 4.53 L/s (0.160 ft³/s), 1-hour operation, and (f) 5.72 L/s (0.202 ft³/s), 1.5-hour operation. Photo P801-D-78810

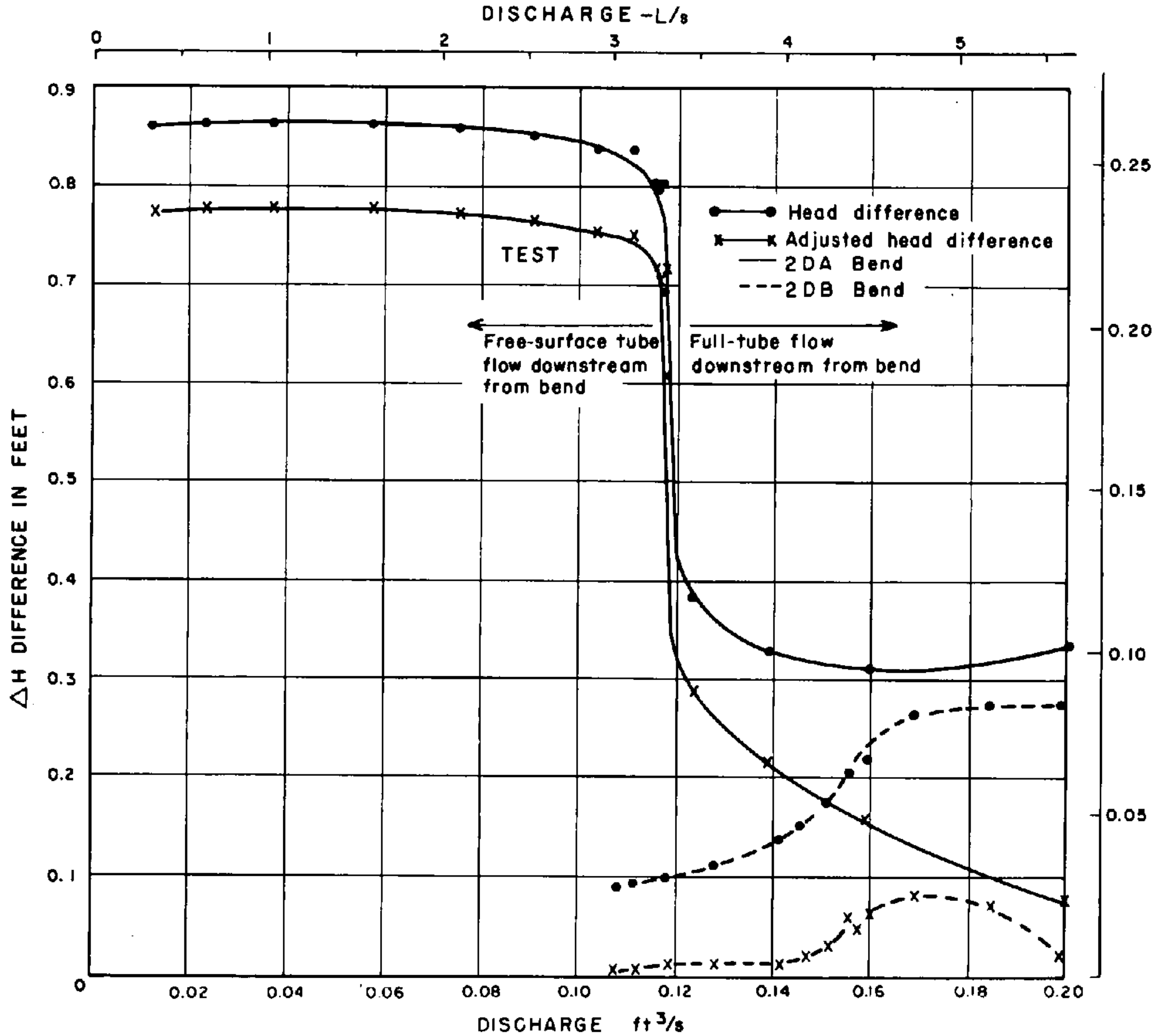

Figure 23.–Head difference versus discharge, bends 2DA and 2DB, $S = 0.005$.

about equal to the bend offset. Yet siphoning occurred for discharges greater than full-tube flow, lowered the upstream gradeline, and mitigated the detrimental effect of the bend.

Observations of Air Entrapment

No appreciable air entrapment had occurred until making tests described in the "Other Flow Depth Tests" section. These tests were with the 2DA and 2DB bends at a 0.005 slope and an air cavity was entrapped in each case for a discharge condition near full-tube flow 3.40 L/s (0.12 ft³/s) for the 0.005 slope (fig. 13). Air cavity effect was a lowering of the upstream hydraulic gradeline for the 2DA bend and a raising for the 2DB bend (fig. 23).

For the 2DA bend the air cavity was in the downstream leg of the bend (fig. 22) and for the 2DB bend, upstream (fig. 25). As discharges were progressively increased for each test series, a greater portion of the entrapped air cavity was purged from the system. The purging action occurred at the downstream end of the cavity where small air bubbles were entrained into the flow, thus removing air from the cavity. For conditions of a tranquil air-water interface for the cavity, air removal was slower, 2DB bend tests/discharges 4.02, 4.28, and 5.64 L/s (0.142, 0.151, and 0.199 ft³/s) of figure 25. When a hydraulic jump condition was present, air removal was more pronounced. However, in either bend and for the maximum 5.66 L/s

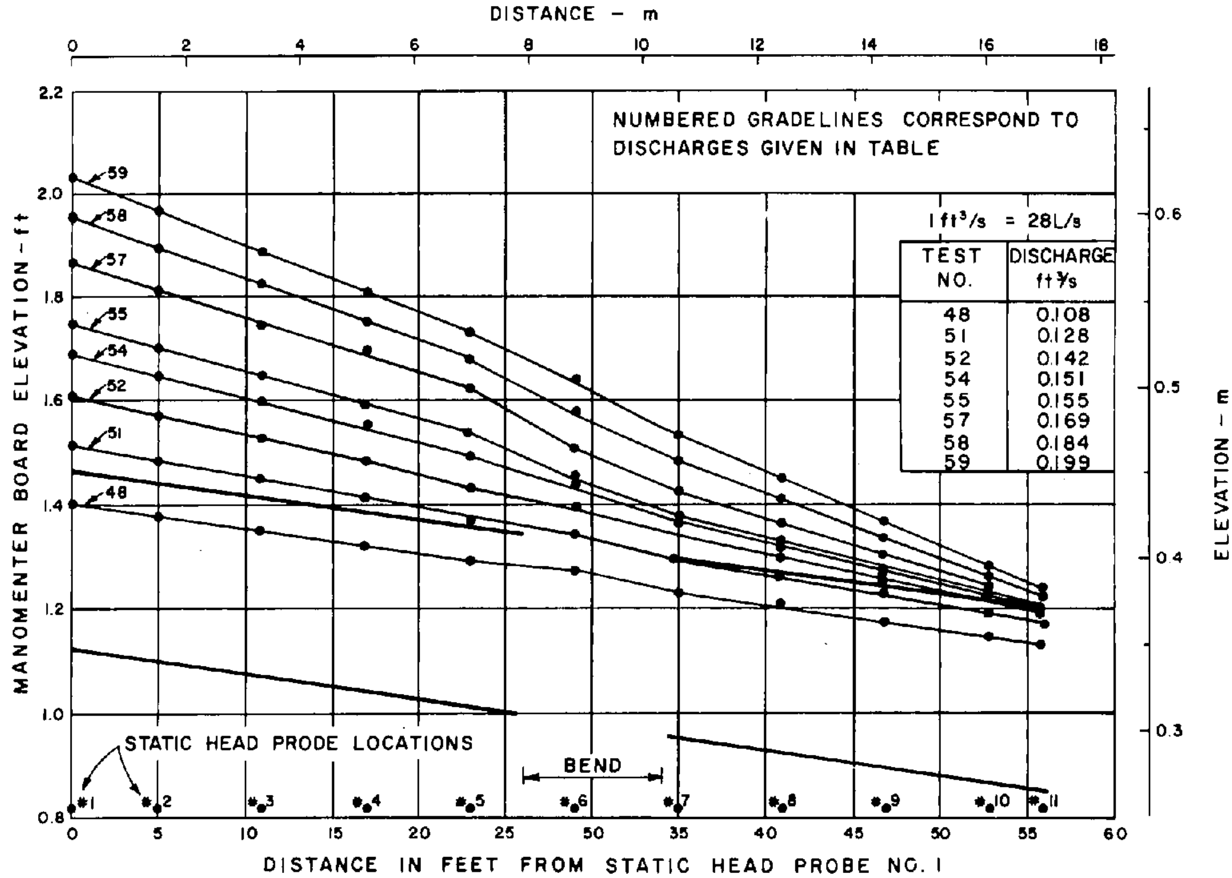

Figure 24.–Hydraulic gradelines for 2DB bend, $S = 0.005$.

(0.2 ft³/s) discharge, a small portion of the entrapped air cavity remained.

Sometime later it was questioned why the entire air cavity was not purged from the system. Small entrained air bubbles were observed rapidly moving downstream when looking through the tubing, and thus it was expected the entire cavity should be purged. Therefore, another test was made with the 2DA bend using a 5.66-L/s (0.2-ft³/s) discharge. Initially, a decrease of the air cavity size was very noticeable, but after 10 to 20 minutes of operation, it appeared to reach stability. A close examination showed the small bubbles were carried a short distance downstream, rose to the crown of the tubing, recombined into large bubbles, and because of their buoyancy the large bubbles moved upstream to be returned to the air cavity (fig. 26). Thus, a process of cyclic air movement within the bend prevented entire purging of the entrapped air cavity. This process was occurring 6 hours later (fig. 26f).

Some additional tests were directed toward entrapped air cavities but were considered inconclusive. This information and a question about the test facility representing a field installation drain are included in appendix 2.

SEDIMENTATION TESTS

Introduction

One consequence of bends is that flow velocities are changed from those of a straight tube and may provide a location for sediment problems. Therefore, one part of this study was to make sedimentation tests with bends. In approaching this problem, it was decided to make sedimentation tests leading up to the bend test. The intent was to gain information for defining a stringent bend test condition. Rationale and results of the test program are given in the following text and a more detailed description in appendix 3.

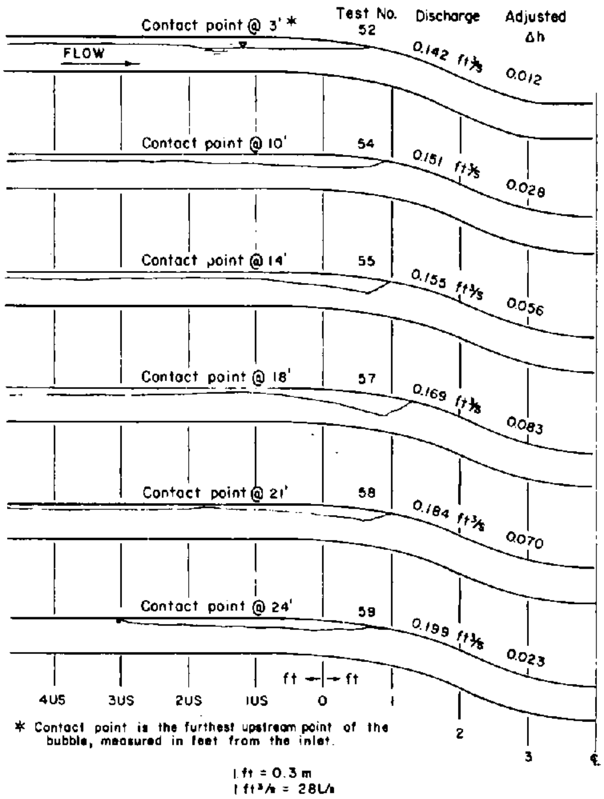

Figure 25.–Water surface profiles in the 2DB bend, $S = 0.005$.

Sediment Injection Procedure

A uniform sand with a 0.2-mm mean diameter was used for the sedimentation tests (fig. 27). For the first test a short length of rubber garden hose was inserted into the tubing at the head box location and extended 1 m (3 ft) downstream from the inlet. A sand-water mixture was funneled into the hose, entered the tubing, and then settled upon the tubing invert. One bad feature was dispersion of the sand-water mixture from the end of the hose, and test observations showed it would take an excessively long time for the sediment to reach the bend. Therefore, two permanent injection tubes were placed at stations 3 and 25, downstream from the inlet and upstream from the bend test section (fig. 3). A hole was cut in the top of the drain tubing and a vertical 25-mm (1-in) diameter transparent plastic tube placed over the hole (fig. 29). With the use of a funnel and the injection tube, sand was dropped dry or settled through water into the drain tubing.

General Characteristics of Sediment Movement

Three series of preliminary-type tests were made to determine flow velocities for incipient sediment movement and velocities which readily moved the sediment.

The first series was made with full-tube flow to determine what average water velocity (discharge divided by tube area) moved the sediment. Movement of the sand grains was observed at a 0.20-m/s (0.66-ft/s) velocity and a 0.23-m/s (0.75-ft/s) velocity moved the leading edge of the sediment deposit 0.53 m (1.75 ft) during a 1-hour interval. Thus, this test series showed that a 0.001 tubing slope was a critical test condition. Note in figure 12 that slopes greater than 0.001 have velocities exceeding the 0.20-m/s (0.66-ft/s) velocity required for moving the sand.

The second series was made for free-surface flow at a 0.001 tube slope and at one-fourth, one-half, and three-fourths flow depths. For the one-fourth flow depth the sediment deposit moved at a rate of 0.08 m/h (0.25 ft/h), for the one-half flow depth a rate of 0.23 m/h (0.75 ft/h), and for the three-fourths flow depth, a rate of 0.61 m/h (2 ft/h). Thickness of the sand deposits varied from 0.1D to 0.2D for the one-fourth flow depth and traveled in sand dunes with a 0.1D to 0.3D height for the other two flow depths. Depths of the sediment were estimated by viewing heights of the deposit through the side of the tube with a scaled template placed against the tube (fig. 28). Marked lines on the template were made at one-tenth intervals of the inside tube diameter. The sediment provided flow resistance and the water surface elevation in the head box was 0.12 mm (0.04 ft) higher than for the normal free-surface flow condition without sediment.

This test series showed the 0.001 tube slope was sufficient to move the sedimentation sand, and the rate of movement increased with the flow depth.

The third series was made with full-tube flow to determine sediment movement with average flow velocities that readily moved the sediment. At 0.32 m/s (1.05 ft/s) water velocity, the rate

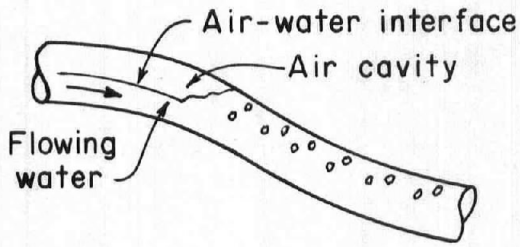

(a) Entrainment of small air bubbles

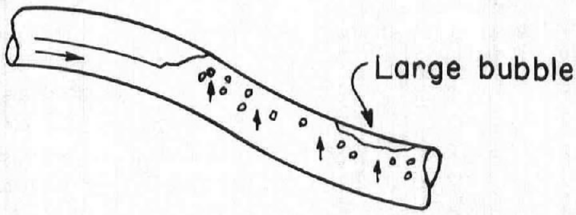

(b) Formation of large air bubble

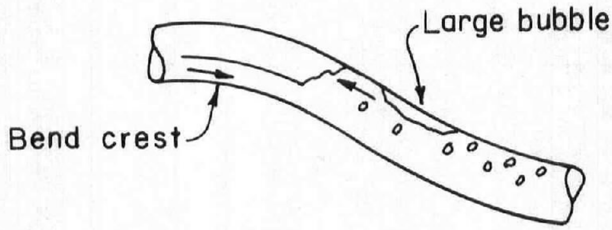

(c) Buoyant force moves large bubble upstream

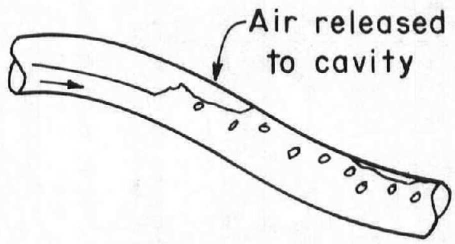

(d) Air from large bubble is returned to air cavity

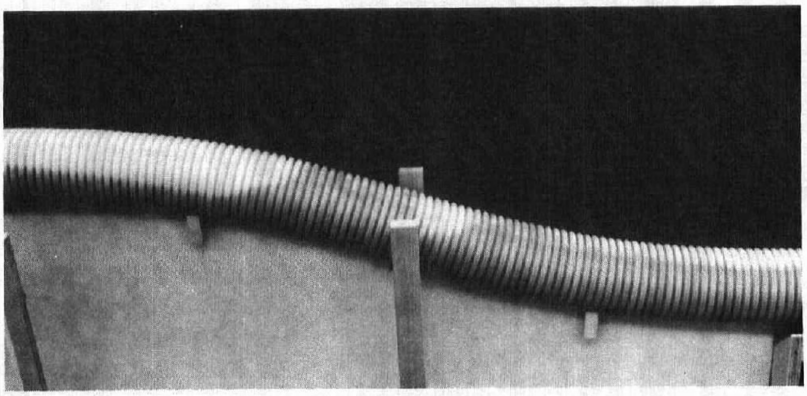

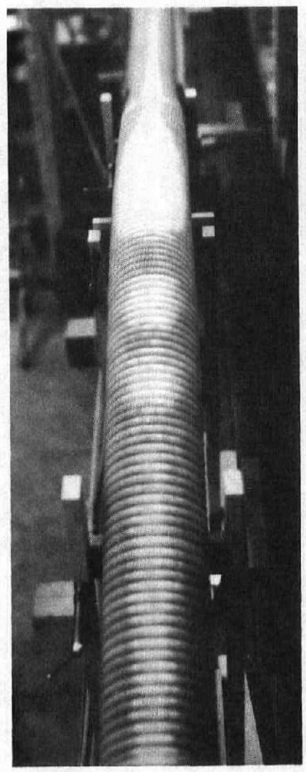

(e) Above–Air bubble moving upstream to the air cavity. Bubble formed near exit of bend, 5.7 L/s (0.2 ft³/s).

(f) Right–Two bubbles moving upstream to the air cavity, 5.7 L/s and 6 hours' operation.

Figure 26.–Cyclic movement of air within the 2DA bend. Photo P801-D-78811

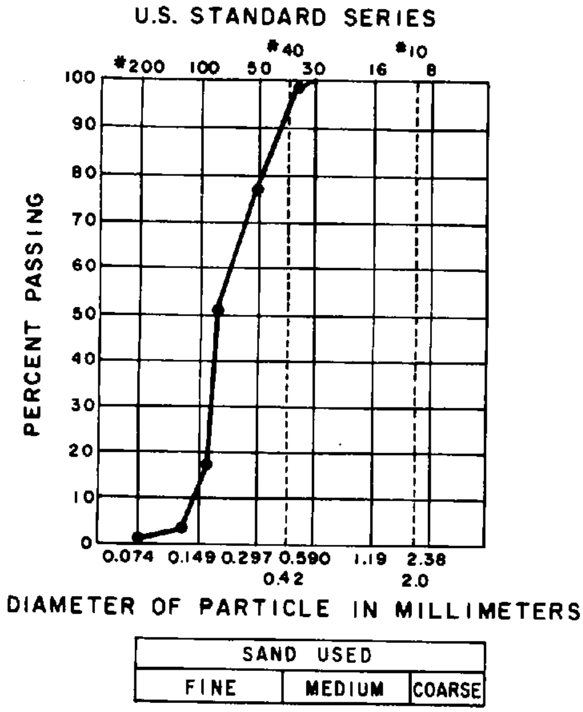

Figure 27.–Sieve analysis of sedimentation sand.

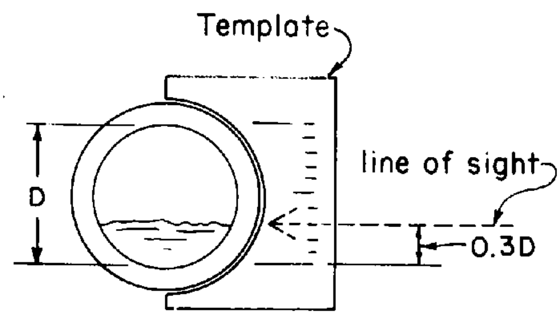

Figure 28.–Schematic showing template method for measuring sediment depth.

of dune movement was 1.2 m/h (4 ft/h) and at 0.37 m/s water velocity, the rate was 3.7 m/h (12 ft/h). Thus, in this velocity range, a relatively small increase in water velocity produced a large increase in the sand dune movement.

When finishing a given sediment test series, the sand was removed from the tube. A 0.67-m/s (2.2-ft/s) flow velocity readily flushed sediment from corrugations and through the tube.

Pyramid Sediment Deposit

A sediment deposit shaped like a pyramid was placed in the drain tubing (fig. 29a). The intent was to simulate a condition of sediment entering a puncture in top of the tubing, completely blocking the flow area, and then reacting to increased drain discharges of a summer's irrigation season. An 18-mm (0.06-ft) differential head gradually built up between the hydraulic gradeline upstream and downstream from the deposit; then water broke through, eroding a passageway near the top of the drain tube (fig. 29b). As the discharges were progressively increased, the area of the flow passageway increased (figs. 29c through 29f).

Thus, the pyramid sediment deposit did not permanently block the waterflow. A 0.17-L/s (0.006-ft^3/s) discharge (for a one-fourth flow depth at 0.0001 tube slope, (fig. 13) was sufficient to break through the deposit. Further, the simulated increased discharges of a summer's drain operation provided a self-cleaning process for the sediment deposit. Higher discharges produced a higher flow velocity in the passageway above the sediment deposit. Thus erosion occurred, the passageway flow area increased, reducing the passageway flow velocity until insufficient to scour the sand.

Lengthwise Sediment Deposit

The intent was to simulate a condition of sediment entering a puncture in the top of the tubing during a low discharge and then reacting to increased drain discharges of a summer's irrigation season. As sediment was slowly injected, a lengthwise sediment deposit formed (fig. 30a). Dashed lines were placed at the top of the sediment deposit because the flow passageway was narrow and did not readily show on the photograph. If sediment injection was too fast, then sand blocked the passageway until sufficient head built up to break through.

Erosion of the sediment deposit readily occurred (figs. 30a through 30e); however, movement of the deposit was extremely slow (fig. 31). The sediment deposit provided resistance to the flowing water, hydraulic gradelines of figure 32. To show the change of the resistive effect, a differential head ΔH was obtained between static head probes No. 5 and 6 for the start and

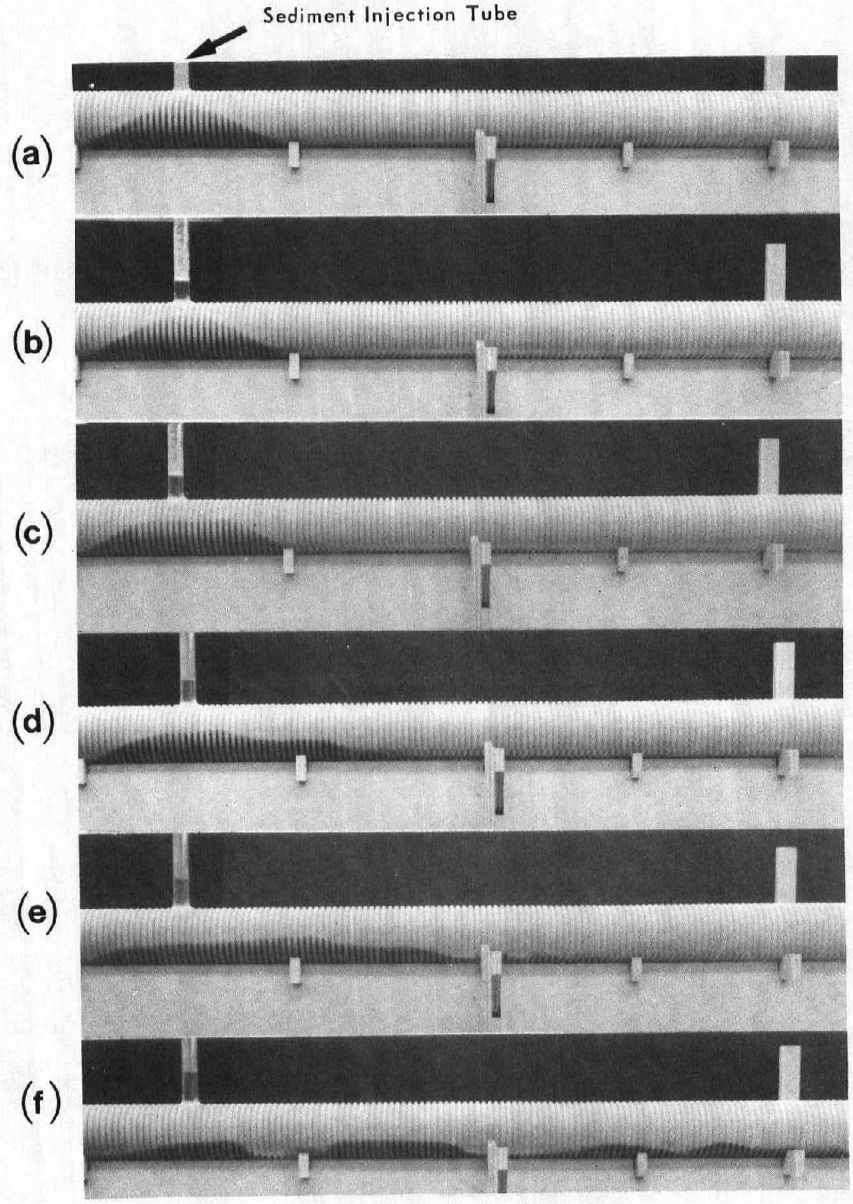

Figure 29.–Sedimentation tests with a pyramid-shaped sediment deposit. Operation times are for each individual test discharge. (a) Before test, (b) Discharge 0.17 L/s (0.006 ft^3/s), 0.5-hour operation, (c) Discharge 0.40 L/s (0.014 ft^3/s), 4-hour operation, (d) Discharge 0.71 L/s (0.025 ft^3/s), 7.5-hour operation, (e) Discharge 1.16 L/s (0.041 ft^3/s), 15-hour operation, and (f) Discharge 1.50 L/s (0.053 ft^3/s), 8-hour operation. Photo P801-D-78812

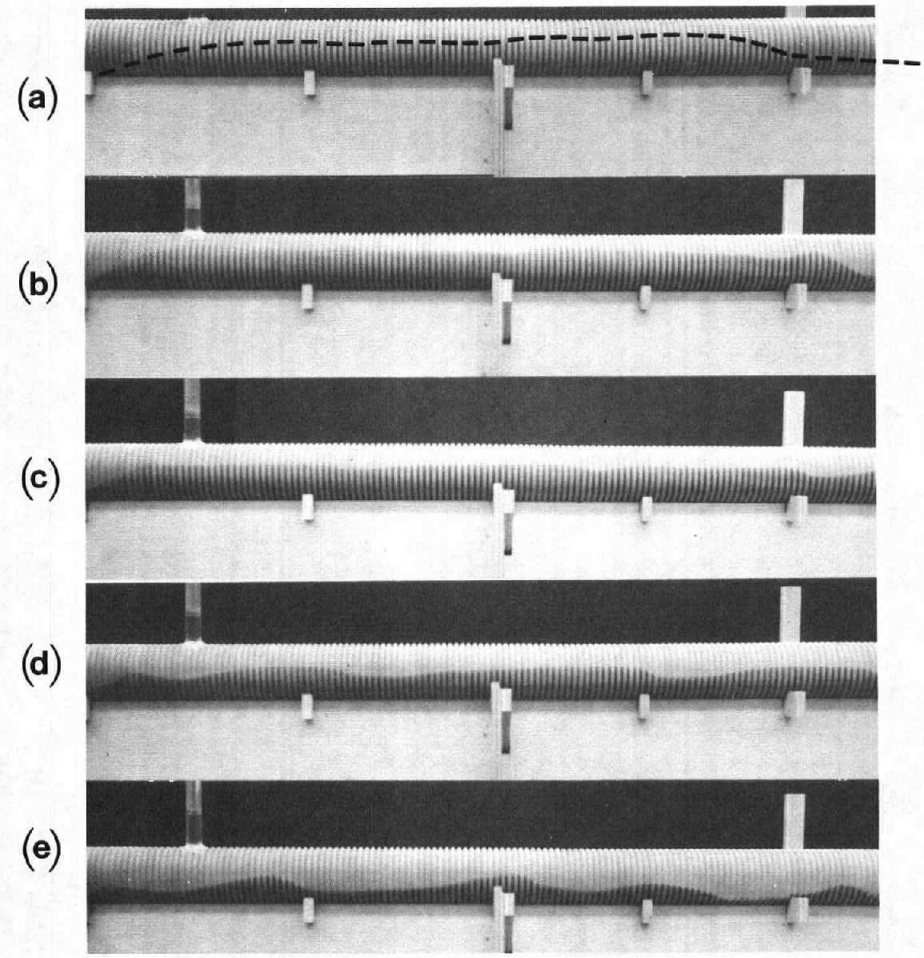

Figure 30.–Sedimentation tests with a lengthwise sediment deposit. (a) After placing sediment in tube, discharge 0.20 L/s (0.007 ft³/s). (b) Discharge 0.20 L/s, 18-hour operation, (c) Discharge 0.40 L/s (0.014 ft³/s), 24-hour operation, (d) Discharge 0.71 L/s (0.025 ft³/s), 32-hour operation, and (e) Discharge 1.10 L/s (0.039 ft³/s), 23-hour operation. Photo P801-D-78813

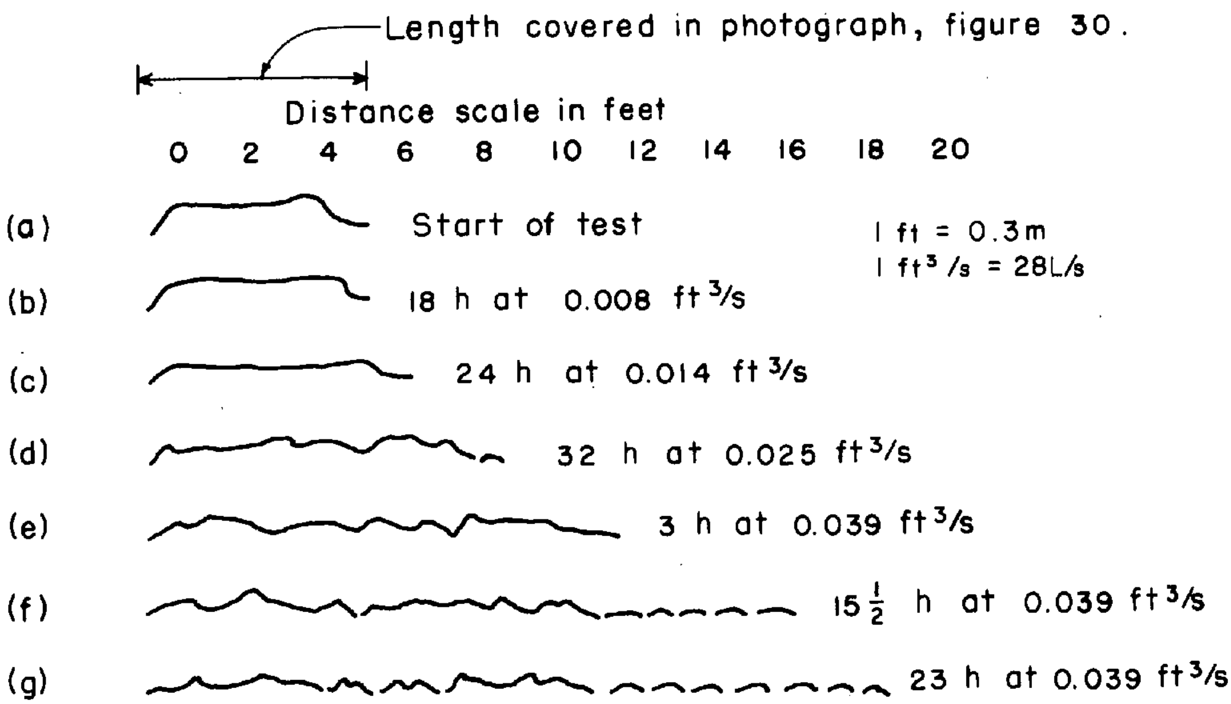

Figure 31.–Schematic showing distance of sediment movement for the lengthwise sediment deposit tests.

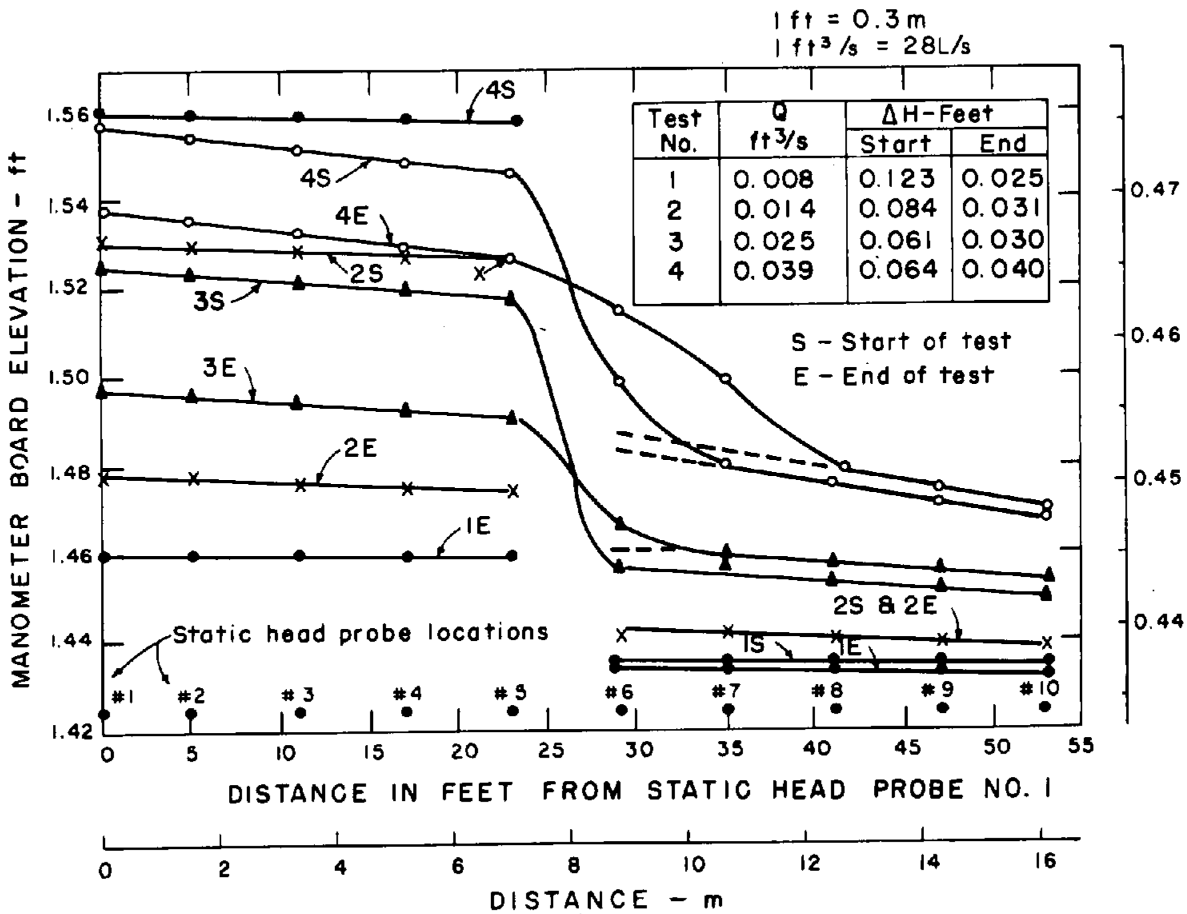

Figure 32.–Hydraulic gradelines for lengthwise sediment deposit.

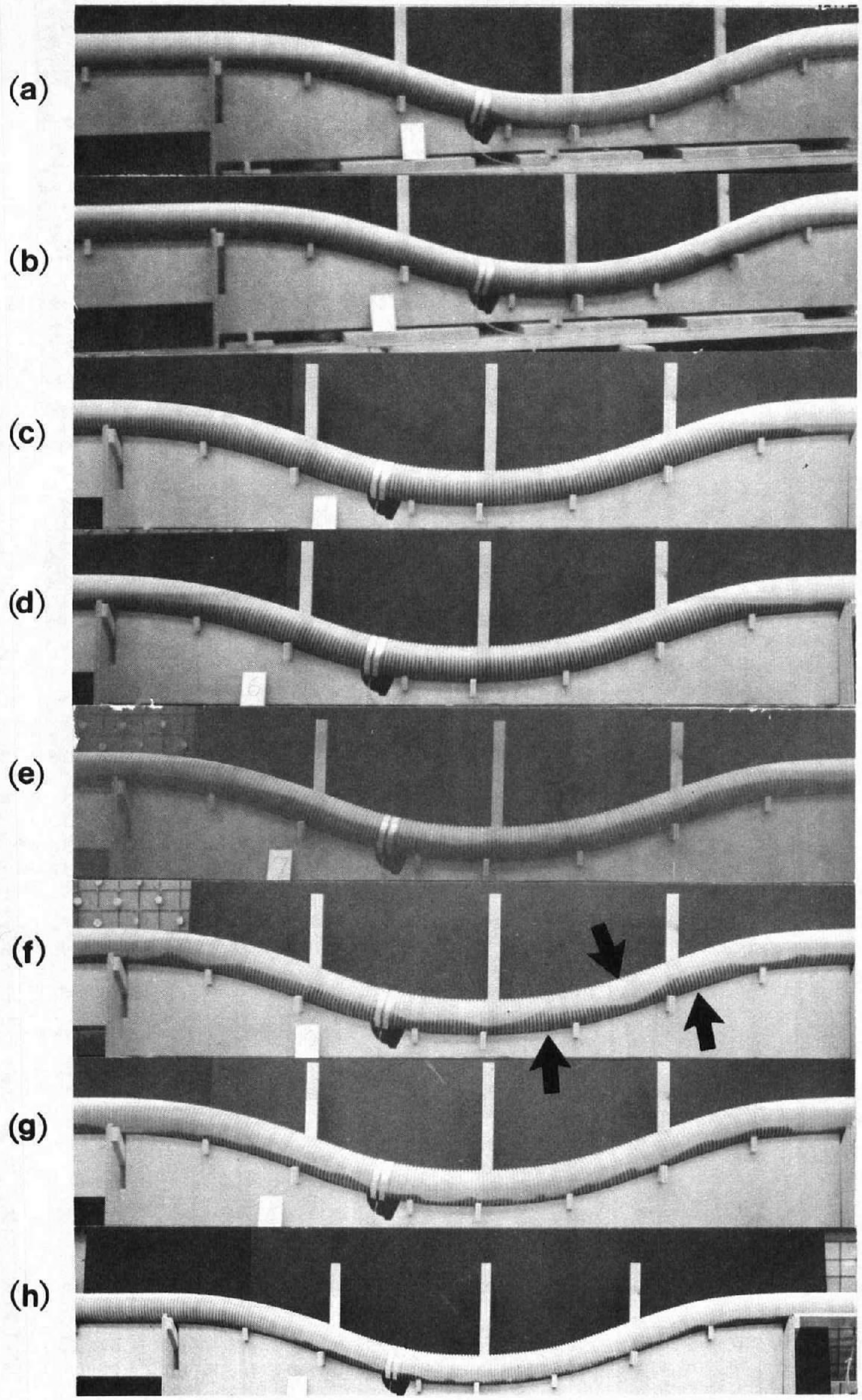

Figure 33.–Sedimentation tests in the 2DB bend, (a & b) Sediment moving into bend during sediment injection, (c) Discharge, 0.17 L/s (0.006 ft³/s), 2-hour operation, (d) Discharge 0.17 L/s, 65-hour operation, (e) Discharge 0.74 L/s (0.026 ft³/s), 0.5-hour operation, (f) Discharge 0.74 L/s, 122-hour operation, (g) Discharge 1.10 L/s (0.039 ft³/s), 72-hour operation, and (h) Discharge 1.53 L/s (0.054 ft³/s), 100-hour operation. Photo P801-D-78814

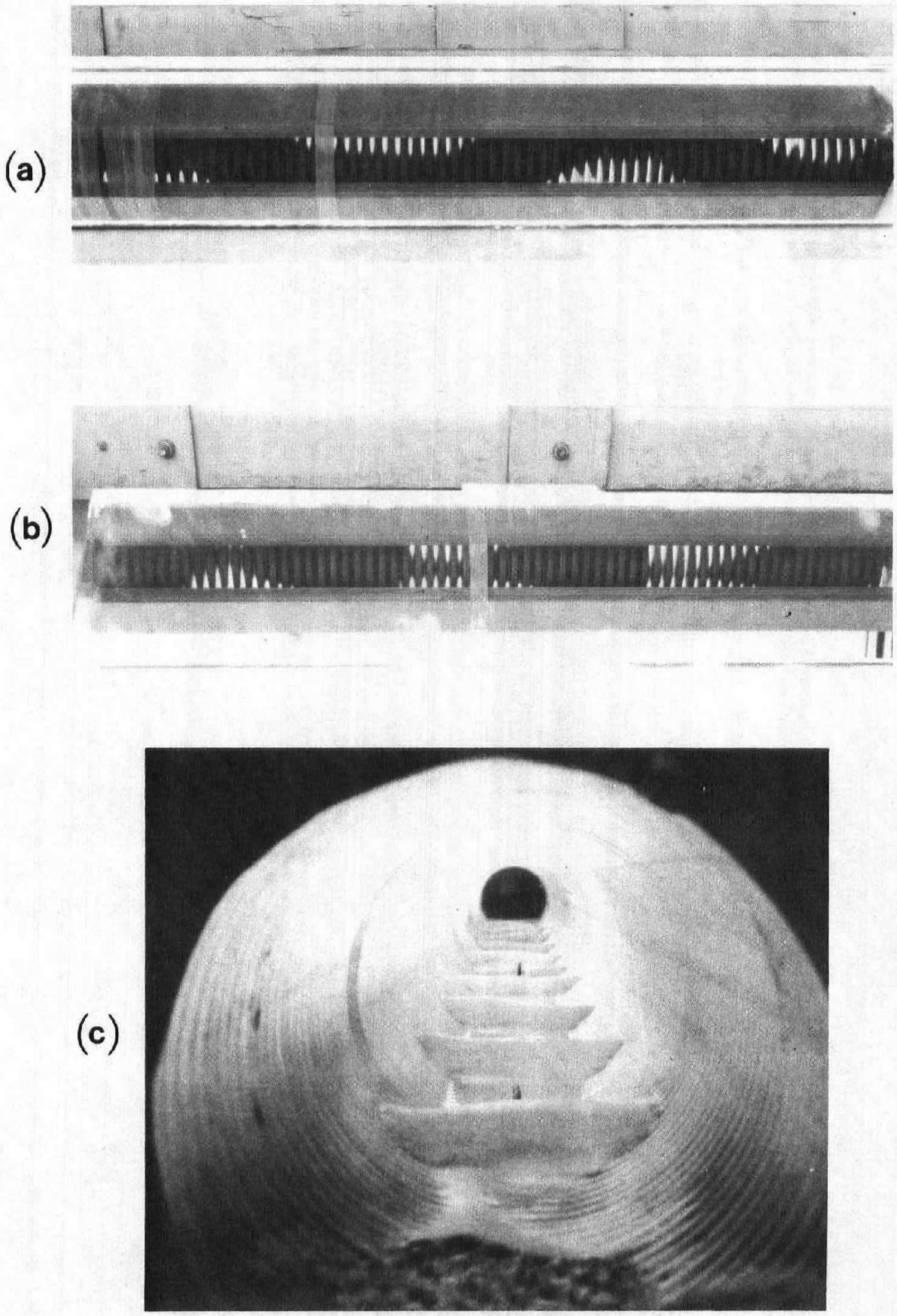

Figure 34.–Shapes of the sediment deposit in the tube downstream from the 2DB bend. (a) View looking up at the tube bottom showing meandering of sediment deposit, discharge 1.10 L/s (0.039 ft^3/s) 45-hour operation, (b) View looking up at tube bottom, sand dunes, discharge 1.53 L/s (0.054 ft^3/s) 100-hour operation, and (c) View looking upstream from the tail box after end of the 2DB bend sedimentation tests. Photo P801-D-78815

end of each test discharge; see figure 32 table. When changing to a new discharge, the resistance was greatest, and then as a larger passageway was eroded, the resistance decreased.

A self-cleaning process occurred similar to the pyramid deposit tests. Also, the lengthwise sediment deposit exhibited a nonclogging tendency. When injecting sediment, the deposit depth increased until passageway flow velocities were sufficient for transporting sand through the passageway and thus preventing total blockage of the waterflow.

Sediment Deposit in the 2DB Bend

A two-diameter offset bend was believed more susceptible to sedimentation problems than a one-diameter offset bend, and the 2DB bend was selected for the test. The 2DB bend would have free-surface flow upstream and downstream from the bend; whereas, the 2DA bend would have a high velocity readily moving sediment in the downhill leg of the bend. A flow condition of one-fourth flow depth and 0.001 tube slope with a 0.17-L/s (0.006-ft³/s) discharge was selected for beginning the test series. Even though previous sedimentation tests showed sediment movement for this flow condition, it was considered a minimal flow for field operation, and therefore a realistic test condition.

Sand was injected 0.6 m (2 ft) upstream from the bend, at a rate slow enough to prevent raising the upstream water level above the three-fourths flow depth. After 2 hours' injection, the sand had traveled into the bend (fig. 33a), and when the sediment deposit was moving along the uphill leg of the bend (fig. 33b) (after about 5 hours), sand injection was stopped. As discharges were progressively increased during the test series, sand was removed from the bend (figs. 33c through 33h) and transported downstream from the bend (figs. 34a and 34b). Flow resistance of the sediment deposit is shown by the hydraulic gradelines of figure 35 and ΔH of the table is head difference between probes No. 5 and 10, with an adjustment made for distance between probes. The test series was concluded after operating 362 hours, and sand was still existing from the tubing into the tail box.

TEST NO.	Q ft³/s	Δ H-FEET START	Δ H-FEET END
1	0.006	0.21	0.10
2	0.026	0.13	0.04
3	0.039	0.06	0.02
4	0.054	0.04	0.02

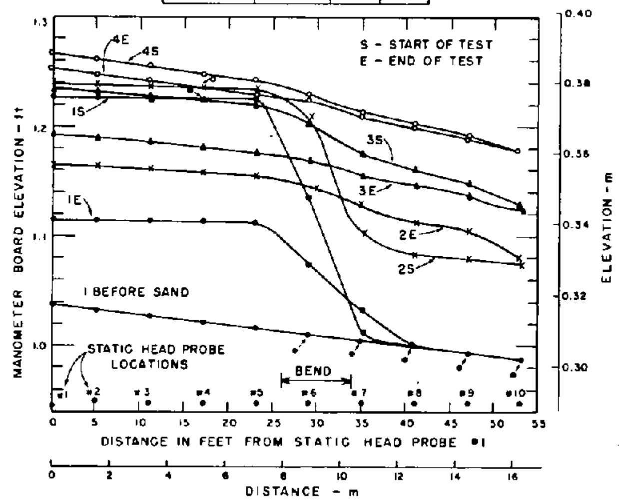

Figure 35.–Hydraulic gradelines for 2DB bend sediment deposit test.

Results of the 2DB sediment tests were similar to those of the pyramid and lengthwise sediment deposit. There was a nonclogging tendency. Sand was transported into the bend, deposited, which formed a small passageway flow area, and provided high velocities transporting sand through the bend. Then as discharges were increased, the self-cleaning process occurred, flushing sediment from the bend. The uphill leg of the bend did not unduly resist sand movement through the tubing. Although more force is required to move particles uphill, the test results did not show a detectable sediment deposit thickness between uphill and downhill legs of the bend. Thus, it was concluded the 2DB bend would pass fine sedimentation sand through the tubing without stopping the waterflow.

APPENDIXES

APPENDIX 1—TABLES

Table 1.—*Results of the full-tube flow tests*

Test No.	Q (L/s)	V (m/s)	S	n	$N_R \times 10^3$	f
1	5.73	0.665	0.014 39	0.015 95	66.4	0.066 9
2	5.58	.647	.013 72	.016 01	64.5	.064 7
3	5.38	.624	.012 78	.016 02	62.3	.067 6
4	5.04	.585	.011 42	.016 16	58.4	.068 8
5	4.84	.562	.010 29	.015 97	56.1	.067 1
6	4.53	.525	.008 96	.015 93	52.5	.066 7
7	4.16	.483	.007 51	.015 87	48.2	.066 3
8	3.85	.447	.006 32	.015 74	44.6	.065 2
9	3.51	.407	.005 13	.015 56	40.7	.063 7
10	3.20	.371	.004 24	.015 51	37.1	.063 2
11	2.94	.342	.003 58	.015 49	34.1	.063 1
12	2.74	.318	.003 06	.015 40	31.7	.062 4
13	2.55	.296	.002 62	.015 33	29.5	.061 8
14	2.33	.271	.002 21	.015 36	27.0	.062 0
15	2.07	.240	.001 73	.015 32	24.0	.061 7
16	1.84	.214	.001 36	.015 26	21.3	.061 4
17	1.67	.194	.001 16	.015 57	19.4	.063 7
18	1.48	.198	.000 88	.015 36	17.1	.062 1
19	1.27	.147	.000 67	.015 55	14.7	.063 5
20	1.08	.125	.000 49	.015 72	12.5	.064 8
21	0.85	.098	.000 31	.015 81	9.8	.065 8

Date: May 8, 1973

Test No.	Q (L/s)	V (m/s)	S	n	$N_R \times 10^3$	f
1	5.49	0.636	0.013 18	0.015 95	67.2	0.067 0
2	5.31	.615	.012 36	.015 98	64.9	.067 2
3	5.06	.586	.010 92	.015 76	61.9	.065 3
4	4.73	.548	.009 51	.015 73	57.9	.065 1
5	4.51	.523	.008 40	.015 49	55.2	.063 2
6	4.22	.489	.007 31	.015 45	51.6	.062 8
7	3.96	.459	.006 37	.015 38	48.4	.062 3
8	3.59	.417	.005 26	.015 39	44.0	.062 3
9	3.32	.385	.004 51	.015 43	40.6	.062 7
10	2.91	.337	.003 38	.015 27	35.6	.061 3
11	2.84	.329	.003 23	.015 28	34.7	.061 4
12	2.58	.299	.002 67	.015 26	31.6	.061 3
13	2.29	.265	.002 08	.015 21	28.0	.060 9
14	2.14	.248	.001 81	.015 19	26.2	.060 7
15	1.97	.229	.001 53	.015 12	24.1	.060 2
16	1.70	.198	.001 15	.015 18	20.8	.060 6
17	1.48	.172	.000 86	.015 08	18.2	.059 8
18	1.29	.150	.000 67	.015 21	15.8	.060 9
19	1.17	.136	.000 55	.015 25	14.3	.061 2
20	0.89	.103	.000 33	.015 66	10.9	.064 5
21	0.76	.088	.000 24	.015 53	9.3	.063 5
22	0.58	.068	.000 15	.015 86	7.1	.066 2
23	0.46	.053	.000 10	.016 73	5.6	.073 6
24	1.38	.171	.000 73	.014 94	16.9	.058 8
25	1.82	.212	.001 30	.015 06	22.3	.059 7
26	2.62	.304	.002 67	.015 02	32.1	.059 4
27	2.84	.330	.003 11	.014 96	34.8	.058 9
28	3.27	.379	.004 14	.015 00	40.0	.059 2

Date: Aug. 6, 1973

Table 2.—*Invert elevations and related manometer board invert readings*

Test slope	0.001	0.001	0.005	0.005	0.01	0.02
Date	May 9	July 6	May 2	May 25	April 17	June 28
Test slope by least squares fit	0.000 869	0.000 929	0.004 64	0.004 82	0.009 60	0.019 6
Probe locations	Invert elevations as reference to a 15-foot bench mark					
1	14.544	14.545	14.708	14.718	14.935	15.374
2	14.537	14.542	14.688	14.694	14.885	15.277
3	14.532	14.535	14.656	14.662	14.826	15.154
4	14.525	14.523	14.623	14.629	14.764	15.032
5	14.523	14.524	14.603	14.605	14.710	14.921
6	14.515	14.517	14.573	14.576	14.651	14.803
7	14.509	14.511	14.545	14.546	14.595	14.685
8	14.507	14.508	14.519	14.519	14.539	14.571
9	14.493	14.497	14.477	14.482	14.466	14.450
10	14.491	14.491	14.457	14.459	14.409	14.330
11	14.483	14.479	14.437	14.438	14.382	14.265
	Manometer board invert readings (see fig. 11)					
1	0.952	0.953	1.116	1.126	1.343	1.782
2	.945	.950	1.096	1.102	1.293	1.685
3	.940	.943	1.064	1.070	1.234	1.562
4	.933	.931	1.031	1.037	1.172	1.440
5	.931	.932	1.011	1.013	1.118	1.329
6	.923	.925	0.981	0.984	1.059	1.211
7	.917	.919	0.953	0.954	1.003	1.093
8	.915	.916	0.927	0.927	0.947	0.979
9	.901	.905	0.885	0.890	0.874	0.858
10	.899	.899	0.865	0.867	0.817	0.738
11	.891	.887	0.845	0.846	0.790	0.673

Metric conversion 1 ft = 0.3048 m

Table 3.—*Results of an individual free-surface tube flow test*

Static head probe location	Measured depth (mm)	V (m/s)	n	$N_R \times 10^3$	f
2	63.1	0.198	0.015 85	21.8	0.063 7
3	62.8	.199	.015 73	21.9	.062 8
4	65.2	.191	.016 66	21.3	.070 0
5	63.1	.198	.015 85	21.8	.063 7
6	63.4	.197	.015 96	21.8	.064 6
7	62.2	.202	.015 50	22.1	.061 1
8	61.3	.205	.015 14	22.3	.058 5
Values obtained from average depth and S = 0.001 095 which are shown in table 4					
	63.1	0.199	0.015 81	21.8	0.063 4

Tubing test slope was S ≈ 0.001 and by least squares fit S = 0.000 929
Individual test discharge 1.08 L/s
Individual slope S = 0.001 095 by least squares fit of water surface elevations at static head probes 2 through 8

Table 4.—*Results of the free-surface tube flow tests*

Test No.	Q (L/s)	Average depth (mm)	V (m/s)	S	n	$N_R \times 10^3$	f
Tests May 9, 1973—test slope S ≈ 0.001—least squares fit S = 0.000 869							
1	1.27	75.9	0.191	0.000 857	0.015 29	22.6	0.057 9
2	1.43	86.3	.188	.000 815	.015 28	22.7	.057 5
3	1.22	75.0	.184	.000 798	.015 23	21.8	.057 5
4	0.84	56.1	.177	.000 899	.015 37	18.3	.061 3
5	0.96	64.1	.175	.000 810	.015 53	19.4	.061 0
6	0.68	49.4	.170	.000 923	.015 44	16.2	.063 5
7	0.41	39.6	.137	.000 863	.016 68	11.1	.078 1
8	1.61	93.6	.198	.001 024	.016 07	23.5	.063 9
Tests July 18 and 19, 1973 (straight configuration of the bend tests)—test slope S ≈ 0.001—least squares fit S = 0.000 929							
1	0.20	26.8	0.116	0.001 018	0.017 48	6.8	0.095 3
2	0.74	52.4	.172	.000 899	.015 47	17.0	.062 9
3	1.41	76.8	.208	.001 054	.015 61	24.7	.060 3

Table 4.—*Results of the free-surface tube flow tests*—continued

Test No.	Q (L/s)	Average depth (mm)	V (m/s)	S	n	$N_R \times 10^3$	f
Tests July 6 and 7, 1973—test slope S ≈ 0.001—least squares fit S = 0.000 929							
1	0.21	28.0	0.115	0.000 970	0.017 37	7.1	0.093 0
2	0.26	31.1	.123	.000 952	.017 13	8.2	.087 8
3	0.35	34.7	.142	.001 125	.017 03	10.4	.084 3
4	0.46	39.9	.154	.001 071	.016 50	12.6	.076 3
5	0.61	45.1	.171	.001 107	.016 09	15.3	.070 4
6	0.81	51.2	.194	.001 214	.015 76	18.9	.065 6
7	0.96	57.3	.199	.001 167	.015 77	20.8	.064 2
**8	1.08	63.1	.199	.001 095	.015 81	21.8	.063 4
9	1.23	67.4	.211	.001 196	.015 91	23.9	.063 6
10	1.36	71.9	.216	.001 196	.015 84	25.1	.062 5
11	1.63	80.2	.231	.001 232	.015 29	27.6	.057 7
12	1.72	88.1	.222	.001 280	.016 24	26.7	.065 0
*13	1.72	94.8	.210	.001 476	.018 16	24.7	.081 8
*14	1.71	100.6	.201	.001 417	.017 95	22.5	.081 3
15	1.51	95.4	.183	.001 095	.017 91	21.4	.079 7
16	1.57	101.8	.183	.001 208	.017 95	20.2	.081 8
17	1.48	99.7	.175	.001 071	.018 11	19.8	.082 4
18	1.31	73.2	.204	.001 089	.016 04	23.8	.063 9
19	1.47	80.5	.207	.001 089	.016 05	24.8	.063 5
20	1.50	83.5	.204	.001 083	.016 28	24.5	.065 2
21	1.54	84.4	.207	.001 083	.016 05	24.9	.063 4
22	1.57	85.0	.210	.001 107	.015 97	25.3	.062 8
23	1.63	88.7	.209	.001 131	.016 20	25.1	.064 7
24	1.64	93.9	.202	.001 268	.017 56	23.9	.076 4
25	1.65	97.8	.197	.001 327	.018 10	22.7	.081 9
26	1.26	71.6	.201	.001 089	.016 19	23.3	.065 3
27	1.14	67.0	.195	.001 054	.016 08	22.1	.065 0
28	1.05	65.2	.186	.000 958	.015 93	20.8	.064 0
29	0.91	59.7	.180	.000 994	.016 33	19.2	.068 3
30	0.83	53.9	.184	.001 071	.015 93	18.6	.066 2
31	0.68	47.8	.177	.001 071	.015 65	16.5	.065 7
32	0.55	43.6	.163	.001 060	.016 27	14.2	.072 6
33	0.48	40.5	.155	.001 077	.016 58	12.8	.076 8
34	0.38	40.5	.137	.000 970	.017 06	10.6	.083 0

* Full tube flow occurring within some portion of the tube.

** Results of this test at static head probes, No. 2 through 8, are shown in table 3.

Table 4.—*Results of the free-surface tube flow tests*—continued

Test No.	Q (L/s)	Average depth (mm)	V (m/s)	S	n	$N_R \times 10^3$	f
Tests May 2, 1973—test slope S ≈ 0.005—least squares fit S = 0.004 64							
1	5.72	Full	0.663	0.014 19	0.015 89	65.6	0.066 4
2	5.49	Full	.637	.013 21	.015 96	63.0	.067 0
3	4.96	Full	.575	.010 73	.015 95	56.8	.066 9
4	4.37	Full	.507	.008 31	.015 90	50.2	.066 6
5	4.05	Full	.469	.007 11	.015 89	46.4	.066 4
6	3.54	91.1	.444	.005 99	.017 47	53.1	.075 3
7	3.23	82.6	.442	.005 49	.016 89	53.2	.070 2
8	3.33	84.1	.448	.005 54	.016 75	53.9	.069 1
9	2.78	72.8	.434	.005 14	.016 33	50.7	.066 3
10	2.34	63.4	.429	.004 88	.015 60	47.3	.060 9
11	1.98	56.4	.418	.004 74	.015 02	43.3	.058 4
12	1.76	53.0	.401	.004 80	.015 36	40.0	.061 9
13	1.19	43.0	.357	.004 70	.015 50	30.8	.066 1
14	0.74	34.4	.299	.004 66	.016 43	21.8	.078 6
15	0.44	27.1	.247	.004 68	.017 51	14.8	.095 3
16	0.35	24.7	.227	.004 70	.018 10	12.6	.104 6
Tests May 25, 1973—test slope S ≈ 0.005—least squares fit S = 0.004 82							
1	0.27	21.3	0.215	0.004 91	0.017 82	10.4	0.106 0
2	0.39	25.3	.245	.004 82	.017 13	13.7	.093 2
3	0.61	30.5	.290	.004 79	.016 11	19.2	.078 1
4	1.18	42.7	.358	.004 75	.015 45	30.7	.065 8
5	1.62	50.9	.391	.004 54	.015 05	37.9	.059 9
6	2.10	59.4	.415	.004 58	.015 19	44.3	.059 1
7	2.89	75.3	.435	.004 74	.015 75	51.4	.061 4
8	3.21	83.8	.433	.005 00	.016 46	52.1	.066 7
9	3.29	91.4	.411	.004 88	.017 00	49.1	.071 4
10	3.29	93.0	.407	.004 88	.017 15	48.3	.072 8
11	3.08	84.1	.414	.004 83	.016 91	49.9	.070 4
12	2.85	75.0	.430	.004 91	.016 20	50.8	.065 0
13	2.52	67.4	.431	.004 79	.015 56	48.9	.060 8
14	2.31	62.8	.429	.004 82	.015 32	47.1	.059 6
15	1.87	54.9	.409	.004 80	.015 30	41.6	.060 9
16	1.40	46.3	.379	.004 77	.015 27	34.6	.062 9
17	0.98	38.7	.339	.004 80	.015 67	27.0	.069 3

Table 4.—*Results of the free-surface tube flow tests*—continued

Test No.	Q (L/s)	Average depth (mm)	V (m/s)	S	n	$N_R \times 10^3$	f
Tests April 26, 1973—test slope S ≈ 0.01—least squares fit S = 0.009 60							
1	4.97	93.0	0.614	0.010 74	0.016 84	72.9	0.070 2
2	4.53	82.9	.619	.009 87	.016 17	74.5	.064 4
3	4.27	77.7	.622	.009 81	.015 94	74.1	.062 8
4	4.50	80.8	.631	.009 88	.015 85	75.7	.061 9
5	4.67	84.1	.631	.009 90	.015 91	75.9	.062 3
6	4.77	86.3	.630	.010 01	.016 05	75.6	.063 5
7	4.96	91.1	.623	.010 24	.016 29	74.4	.065 5
8	5.01	91.7	.625	.010 24	.016 22	74.4	.065 0
9	5.01	Full	.581	.011 07	.016 03	57.4	.067 6
10	5.01	Full	.581	.011 30	.016 20	57.4	.069 0
11	5.00	95.0	.609	.010 88	.017 01	71.6	.071 8
12	4.92	92.4	.611	.010 74	.016 96	72.6	.071 1
13	1.27	37.8	.453	.009 44	.016 29	35.6	.075 3
14	0.95	32.9	.410	.009 42	.016 66	28.7	.081 8
15	0.66	27.7	.362	.009 42	.017 19	22.1	.091 2
16	0.49	24.7	.320	.009 46	.018 14	17.6	.105 3
17	0.41	22.9	.297	.009 46	.018 71	15.3	.114 5
Tests June 28, 1973—test slope S ≈ 0.02—least squares fit S = 0.019 6							
1	0.82	26.5	0.479	0.019 69	0.018 23	28.0	0.104 1
2	0.65	24.4	.432	.019 70	.019 23	23.5	.118 7
3	1.13	30.5	.541	.019 75	.017 55	35.7	.092 6
4	1.50	34.4	.609	.019 72	.016 62	44.3	.080 4
5	1.91	39.0	.650	.019 77	.016 65	52.3	.078 1
6	2.46	43.9	.716	.019 73	.016 02	62.8	.070 2
7	2.88	47.8	.748	.019 73	.015 98	69.8	.068 4
8	3.17	50.6	.766	.019 74	.015 99	74.2	.067 7
9	3.50	53.9	.780	.019 80	.016 16	78.7	.068 2
10	3.90	57.3	.806	.019 83	.016 06	84.2	.066 5
11	4.30	61.3	.821	.019 84	.016 11	89.0	.066 2
12	4.71	64.9	.839	.019 84	.016 10	93.7	.065 4
13	5.11	68.6	.854	.019 79	.016 05	97.6	.064 5
14	5.67	73.2	.883	.019 78	.015 77	103.4	.061 8
Tests July 2 and 3, 1973 (straight configuration of the bend tests)—test slope S ≈ 0.02—least squares fit S = 0.019 6							
1	0.82	26.5	0.472	0.019 65	0.018 58	27.8	0.107 8
2	3.38	52.4	.781	.019 75	.015 92	77.4	.066 6
3	5.65	72.8	.883	.019 79	.015 74	103.3	.061 6

Table 5.—*Manometer readings for bend tests at the 0.001 test slope*

Probe location	Straight	2DA bend	1DA bend	1DB bend	2DB bend	Straight
			1/4-flow depth Q = 0.20 L/s			
Headbox	1.048	1.785	1.398	1.046	1.046	1.047
1	1.042	1.784	1.398	1.040	1.040	1.042
2	1.036	1.784	1.398	1.034	1.034	1.036
3	1.030	1.783	1.398	1.028	1.028	1.030
4	1.027	1.783	1.398	1.024	1.024	1.027
5	1.020	1.782	1.397	1.016	1.016	1.021
6	1.014	1.781	1.396	1.013	1.013	1.014
7	1.006	1.007	1.007	1.007	1.007	1.008
8	1.000	1.000	1.001	1.002	1.002	1.002
9	0.993	0.994	0.994	0.995	0.995	0.996
10	0.987	0.988	0.988	0.989	0.990	0.990
11	0.986	0.987	0.987	0.988	0.988	0.988
			1/2-flow depth Q = 0.74 L/s			
Headbox	1.133	1.857	1.461	1.130	1.130	1.132
1	1.126	1.855	1.458	1.123	1.123	1.126
2	1.119	1.852	1.457	1.117	1.117	1.119
3	1.114	1.850	1.455	1.110	1.110	1.114
4	1.109	1.848	1.454	1.106	1.105	1.109
5	1.103	1.847	1.452	1.099	1.098	1.103
6	1.098	1.843	1.448	1.098	1.098	1.098
7	1.092	1.090	1.092	1.091	1.092	1.092
8	1.087	1.086	1.086	1.086	1.087	1.086
9	1.081	1.081	1.081	1.081	1.082	1.081
10	1.077	1.076	1.077	1.077	1.077	1.077
11	1.075	1.075	1.076	1.076	1.076	1.075
			3/4-flow depth Q = 1.41 L/s			
Headbox	1.218	1.918	1.526	1.217	1.218	1.217
1	1.208	1.911	1.518	1.207	1.208	1.207
2	1.201	1.907	1.513	1.200	1.201	1.200
3	1.197	1.901	1.508	1.195	1.196	1.195
4	1.190	1.897	1.503	1.189	1.190	1.189
5	1.183	1.891	1.497	1.182	1.183	1.182
6	1.178	1.884	1.487	1.179	1.180	1.177
7	1.170	1.169	1.170	1.170	1.170	1.170
8	1.164	1.164	1.163	1.164	1.164	1.164
9	1.158	1.157	1.158	1.158	1.158	1.158
10	1.150	1.150	1.150	1.151	1.151	1.151
11	1.148	1.148	1.148	1.148	1.148	1.148

Metric conversion 1 ft = 0.3048 m

Table 6.—*Head differences (ΔH) for bends above grade*

Bend	Flow depth	Test slopes 0.001	0.005	0.02
2DA	1/4	0.235	0.238	0.232
2DA	1/2	.229	.241	.244
2DA	3/4	.216	.232	.247
1DA	1/4	.116	.119	.110
1DA	1/2	.107	.119	.125
1DA	3/4	.094	.110	.128

Vertical offset of the IDA bend was 0.119 m above grade, and the 2DA bend was 0.238 m above grade. Definition and manner of obtaining head differences: The head difference was the ΔH distance between the hydraulic gradeline for the straight tube and tube with bend, figure 1. This ΔH measurement was made at the beginning of the bend which was at the 7.9-m mark on the abscissa scale, see figure 17.

Table 7.—*Adjusted head differences for the 2DA and 2DB bends, $S \approx 0.005$ test slope*

Test No.	Q (L/s)	$\Delta H_{5\text{-}8}$ (m)	V (m/s)	S	ΔH_{sr} (m)	Adjusted ΔH (m)
			Tests–2DA bend			
16	0.37	0.261		0.004 82	0.027	0.235
17	0.67	.263		.004 82	.027	.236
18	1.10	.263		.004 82	.027	.236
19	1.63	.263		.004 82	.027	.236
20	2.13	.261		.004 82	.027	.235
21	2.56	.259		.004 82	.027	.232
22	2.95	.256		.004 82	.027	.230
23	3.14	.255		.004 82	.027	.229
24	3.29	.245		.004 82	.027	.218
25	3.33	.212		.004 82	.027	.185
26	3.30	.243		.004 82	.027	.216
28	3.31	.244		.004 82	.027	.218
29	3.49	.115	0.404	.005 16	.028	.087
30	3.96	.100	.459	.006 64	.037	.063
31	4.52	.095	.524	.008 84	.048	.047
32	5.72	.101	.664	.014 40	.079	.023
			Tests–2DB bend			
48	3.05	.028		.004 82	.027	.001
49	3.15	.029		.004 82	.027	.002
50	3.34	.030		.004 82	.027	.004
51	3.61	.034	.419	.005 50	.030	.004
52	4.01	.041	.465	.006 84	.037	.004
53	4.15	.045	.482	.007 40	.041	.005
54	4.28	.052	.497	.007 88	.043	.008
55	4.39	.063	.509	.008 34	.046	.017
56	4.51	.067	.522	.008 80	.048	.019
57	4.78	.080	.554	.010 00	.055	.025
58	5.22	.084	.605	.011 90	.065	.021
59	5.63	.084	.653	.013 92	.076	.007

$\Delta H_{5\text{-}8}$ —Head difference between static head probes No. 5 and 8.

V —Velocity for full-tube flow condition.

S —Slope for computing head difference for straight-tube test condition. For free-surface tube flow $S = 0.004\ 82$ and for full-tube flow S was obtained from figure 9 using V.

ΔH_{sr} —Head loss because of flow surface resistance for a 5.49-m distance between static head probes No. 5 and 8, $\Delta H_{sr} = S \times 5.49$ m.

Adjusted ΔH—Represents a head difference occurring which was greater than would occur for a normal 5.5-m length of straight tube, $\Delta H_{5\text{-}8} - \Delta H_{sr}$ = Adjusted ΔH.

APPENDIX 2–ENTRAPPED AIR

Some additional air entrapment tests were made with the 2DB bend but with a 0.001 test slope. Each test was started in a manner to introduce the maximum size air cavity into the tube. Initially, free-surface tube flow was established; then the tailgate was raised and the supply valve quickly opened. Water level in the head box rose rapidly and a large air cavity was entrapped. In many instances the air cavity was present in the straight tube upstream from the bend. Then the valve was turned back to the desired test discharge. During the initial discharge increase, large slugs of air from the air cavity could be forced through the bend. In some cases when decreasing the discharge, air from the cavity would be expelled upstream along the tube and into the head box. But for discharges tested, an apparent stable air cavity formed after a period of operation (figs. 36a to 36e). The results were similar to those of the 0.005 slope tests, except the air cavity extended slightly further into the bend.

Another test series was made with a constant discharge to observe variation of the air cavity with respect to time (figs. 36f through 36i). Location of the air cavity within the bend changed very noticeably at the beginning of the test series. As air was removed from the air cavity, elevation of the hydraulic gradeline upstream from the bend lowered. There was very little noticeable change in the air cavity during the last hour and 20 minutes of operation time. The cyclic air movement was assumed near a state of equilibrium, and the test series concluded. After the tests, the head difference between static head probes No. 5 and 8 was used in an effort to provide some quantitative measure of whether the process was at equilibrium (fig. 37). The letters on the curve correspond to water surface profiles of figure 36. If equilibrium was achieved, then the curve should asymptotically approach a horizontal line. While the curve through the data points is asymptotically shaped, it appears that after 3.75 hours' operation, equilibrium had not been reached. Many of the previous air entrapment tests operated for an approximate 1-hour period and thus may not have attained complete equilibrium.

The entrapped air cavity was accompanied by siphoning. Siphoning was considered a corrective action for the adverse effect of hump bends because siphoning action lowered the upstream hydraulic gradeline. The process of cyclic air movement within the bend was important with respect to siphoning. This process influenced air removal from the cavity which in turn created a low pressure that produced the siphoning action.

Results of the 2DA bend tests were reexamined and studied with the cyclic air process in mind. The flow velocity and tube slope were considered important factors for the process. High velocity flow moves the small entrained bubbles further downstream before the bubbles can rise to the tubing crown. In figure 22, the higher discharges (also higher velocities) have smaller air cavity size. A greater slope increases the upstream buoyant force component for the large bubbles. Large bubbles formed near the downstream end of the bend. As the bubble grew in size and reached a steeper slope, a portion of the bubble would break off and move upstream. Upstream speed of the bubble increased upon reaching the steeper part of the bend. This was observed for the test condition of figure 26e; note bubble moving upstream at steeper part of the bend. Thus, higher velocities would be required to prevent the upstream bubble movement.

Whether the laboratory test facility bends accurately represented field drain conditions concerning air entrapment was questionable. There would be different flow conditions for bends extending a longer distance, and thus it was not known whether siphoning would develop. Possibly the milder flow would not entrain small bubbles for purging the entrapped air cavity, and then again, because of a very flat slope air, would readily flush from the tubing, similar to that for a straight tube condition. Also, whether entrapped air would occur in a field drain was a matter of controversy. There were two schools of thought: (1) Impossible, because the perforations of the field drain would readily allow entry and exit of air into the gravel envelope; (2) Possible, because air does not readily move through a wet gravel and therefore would be blocked at the gravel envelope.

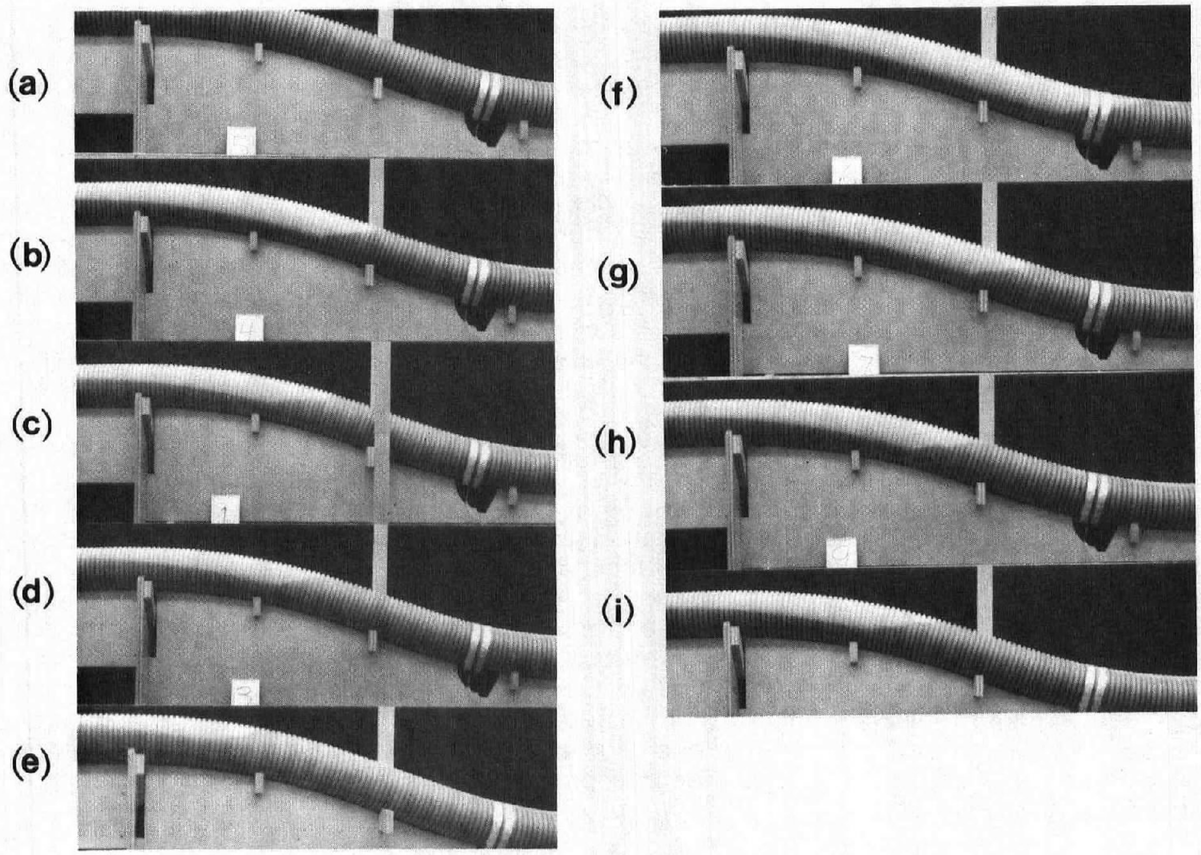

Figure 36.–Water surface profiles, 2DB bend, $S = 0.001$. Left–Variation of the air cavity size with respect to discharge. (a) Discharge 2.61 L/s (0.092 ft³/s) and 0.5-hour operation, (b) Discharge 2.78 L/s (0.098 ft³/s) and 1-hour operation, (c) Discharge 3.54 L/s (0.125 ft³/s) and 2.5-hour operation, (d) Discharge 4.50 L/s (0.159 ft³/s) and 1.25-hour operation, (e) Discharge 5.07 L/s (0.179 ft³/s) and 3.75-hour operation, (f) through (i) Variation of the air cavity size with respect to time for a 3.40 L/s (0.120 ft³/s) discharge, (f) After establishing test conditions, (g) 0.16-h operation, (h) 1.16-h operation, (i) 3.75-hour operation. Photo P801-D-78816

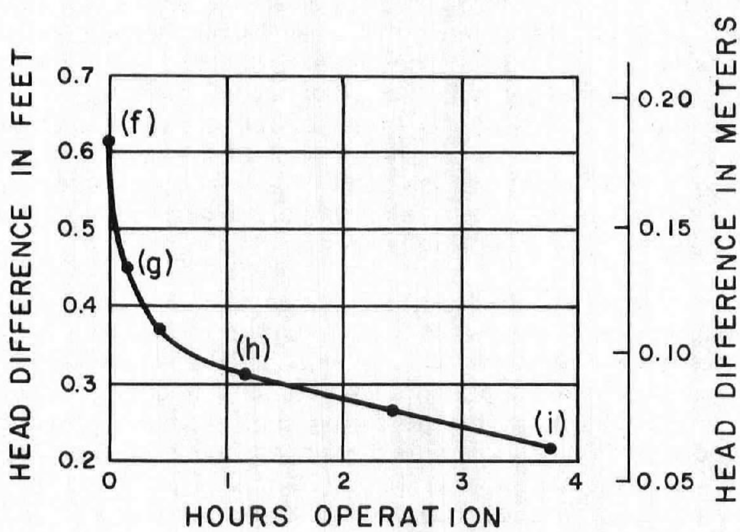

Figure 37.–Head difference versus operation time in the 2DB bend, $S = 0.005$.

While the laboratory tests showed a favorable siphoning condition, it was not certain this siphoning would occur for a field drain. Yet, it was felt worthwhile mentioning these observations. Thus, the drainage engineers who work in the field may consider how representative the tests were, if there are potential benefits to be gained by performing future tests, and if so, a more accurate formation for future laboratory tests.

APPENDIX 3–SEDIMENTATION TESTS

Introduction

Results from non-standardized-type tests are subject to how the tests were performed. The drainage engineer may desire more information so he can judge how representative the laboratory tests are of complex field problems. Therefore, a detailed description of the sediment tests is given.

General Characteristics of Sediment Movement

The first series was made to determine what average water velocity (discharge divided by tube area) moved the sediment. The corrugated plastic drain tube was filled with water. A hose was used to place 1000 cm^3 of sediment along a 0.55-m (1.8-ft) length of the tubing invert. Discharges were then progressively increased and observations made for sediment movement. At a 0.13-m/s (0.43-ft/s) average velocity, there was no apparent sediment movement; at 0.17 m/s (0.57 ft/s) sediment appeared to be on the verge of moving; and at 0.20 m/s (0.66 ft/s) sediment movement was observed at a small hump in the deposit. Observations for these three test velocities were made over a 20-min interval.

Two small dunes formed near the leading edge (downstream end) of the sediment deposit for a 0.23-m/s (0.75-ft/s) velocity. During a 1-hour operation, the leading edge of the sediment deposit moved 0.53 m (1.75 ft) downstream.

After operating 2 hours at a 0.27-m/s (0.87-ft/s) velocity, the sediment deposit was distributed along a 4.4-m (14.5-ft) length. For the first upstream 1.4-m (4.5-ft) length, sediment remained only in the bottom corrugations of the tubing; thus, the 0.27-m/s (0.87-ft/s) velocity was not sufficient to remove sediment from the bottom of the corrugations. From 1.4 to 2.6 m (4.5 to 8.5 ft), there was a series of small dunes, each less than 50 mm (2 in) long and probably less than 12 mm (0.5 in) high. Downstream from the dunes, sediment was deposited only in the bottom corrugations, with diminishing depth in the downstream direction. There was sorting of sediment size. Evidently the flow velocity more readily carried the small sand grains and deposited these grains thinly at the downstream extremity of the deposit.

Observing sediment motion through the translucent, corrugated plastic tubing was difficult. Individual motion of sand grains was generally impossible to see, unless the grains were close to the tube boundary. However, sediment motion in the form of dune movement was easier to detect. Location of a dune could be marked and within a few minutes' movement of the dune could be detected downstream relative to the mark.

The second series was made for free-surface flow. In the first series, a 0.20-m/s (0.66-ft/s) average velocity showed visual movement of the sand grains; from figure 12, tubing slopes greater than 0.001 have average velocities greater than 0.20 m/s and should be sufficient to move the sedimentation sand. The 0.001 tubing slope appeared marginal, and one-fourth, one-half, and three-fourths flow depths were chosen for testing. There was some question concerning the sediment injection rate. If sand was injected too fast, the upstream water surface would be excessively raised. It was decided to put 50 cm^3 of sand every 15 min into both injection tubes, and hope the injection rate would not overly distort the free-surface flow conditions. The injection of sand continued throughout all three flow depth tests.

A one-fourth flow depth was established and then sediment was injected into the tube. During the first hour's operation, movement of the sediment was barely detectable. For the sediment injection tube near the head box, the leading edge of the deposit moved downstream a distance of four corrugations along the tube. For the injection tube near the bend test section, the leading edge of the deposit moved only one corrugation. As the injection continued, the sediment depth increased; the local velocity and sediment movement was faster. After 7 hours' operation, the leading edge of the sediment deposit for the injection tube near the head box moved 0.23 m (0.74 ft) during the last 2-hour interval and 0.13 m (0.43 ft) for the deposit near the bend test section. The sediment deposits were smooth at the beginning of the test, but after 5-1/2 hours' operation, the downstream portion of the deposits had a partial dune formation. Depth of the sand deposits varied from 0.1D to 0.2D. Over the 8.5-hour operation, the water surface elevation in the head box rose 12 mm (0.04 ft) because of increased flow resistance of the sand.

The one-half flow depth tests were continued with the sediment deposits that remained from the previous one-fourth flow depth tests. Data from the "Free-Surface Tube Flow" section were used in setting a one-half flow depth from manometer readings of static head probes located downstream from the second sediment deposit. The rate of sand transport increased rapidly over that of the one-fourth flow depth. After 6 hours' operation, sand dunes having a height of about 0.3D were observed to move downstream about 0.18 to 0.24 m/h (0.6 to 0.8 ft/h). After 10.5 hours' operation, the water surface elevation in the head box was 12 mm (0.04 ft) higher than that for a one-half uniform flow depth with no sediment.

Results of the three-fourths flow depth were similar to those of the one-half flow depth tests, the exception being that downstream movement of the sand dunes varied between 0.24 to 0.61 m/h (0.8 to 2 ft/h).

This second test series showed the normal range of discharges for a 0.001 tube slope moved the sedimentation sand. Even at the one-fourth flow depth the sand was slowly moved, which was contrary to the first series test results, showing 0.20-m/s (0.66-ft/s) velocity for incipient sediment movement. The average velocity for the one-fourth flow depth was slightly less than 0.12 m/s (0.4 ft/s) (fig. 12). However, it was observed that local velocities near the sediment deposit may have been greater than 0.12 m/s. The water level rose upstream from the deposit and the water surface gradient producing flow across the deposit was probably greater than 0.001.

The third series was observations of sediment dune movement with full-tube flow conditions. At 0.32-m/s (1.05-ft/s) water velocity, dunes moved 0.3 m (1 ft) in 15 min, a rate of 1.2 m/h (4 ft/h); and at 0.37-m/s (1.2-ft/s) water velocity, dunes moved 0.6 m (2 ft) in 10 min, a rate of 3.7 m/h (12 ft/h). Thus, in this velocity range, a relatively small increase in water velocity produced a large increase in the sand dune movement.

Pyramid Sediment Deposit

For this test, the intent was to simulate a condition of sediment entering a puncture in the top of the tubing, completely blocking the flow area, and then reacting to increased drain discharges of a summer's irrigation season. Slope of the tubing was 0.001, which was considered a representative field condition for testing. There was 2500 cm^3 of sand forming a pyramid-shaped deposit, and the sand extended above the tubing into the injection tube, figure 29a. The first plan was to inject sand with a one-fourth flow depth free-surface flow condition. However, it was believed the tubing would fill up with water upstream from the deposit and be practically empty on the downstream side. If the water did break through, then the deposit would be easily eroded. Thus, it was decided a full-tube condition was a more conservative test, and sand was injected into the tubing when full of water but not flowing.

A 0.17 L/s (0.006 ft^3/s) discharge was set for one-fourth flow depth and 0.001 tube slope, figure 13. Gradually, an 18-mm (0.06-ft) differential head built up between hydraulic gradelines upstream and downstream from the deposit. Then water broke through the deposit and a passageway was eroded near the top of the drain tube, figure 29b. Thus, the pyramid deposit did not permanently block the waterflow.

The test was continued by progressively increasing the discharge, figures 29c through 29f. Each discharge was maintained until there appeared to be no appreciable sediment movement. When establishing a new discharge, velocity through the passageway increased to erode the sand deposit. Size of the passageway flow area increased as erosion occurred, thereby reducing flow velocity through the passageway. Erosion gradually diminished the passageway velocity and reached equilibrium with scouring velocity of the sand. During the entire test, the downstream edge of the sediment deposit moved 1.1 m (3.5 ft), right edge of figure 29f. No appreciable amount of sand traveled beyond that point.

At the equilibrium condition, the passageway velocity appeared useful for checking the velocity that produced incipient sediment movement. Thus, measurements were made of the passageway depth for computing area and velocity. However, it was difficult to make a judgement about the depth representing equilibrium, especially for conditions in figures 29d and 29e. Sometimes it appeared that the high points were not eroding while some lower points were. Therefore, passageway velocities were computed for the uppermost point and at a lower point where erosion has been observed. Results of the measurements were as follows:

Q	t	D_u	D_l	V_u	V_l
0.17	0.5	0.25D	0.25D	0.10	0.10
0.40	4	.35D	0.40D	.15	.12
0.71	7.5	.43D	0.65D	.20	.12
1.16	15	.55D	0.70D	.24	.18
1.50	8	.75D	1.00D	.22	.18

D–inside diameter of tube, 105 mm (0.344 ft)

where

Q –test discharge, (L/s)

t–hours of operation at discharge Q

D_u–depth of passageway at upper point on deposit

D_l–depth of passageway at lower point on deposit

V_u –passageway velocity for upper point, (m/s)

V_l–passageway velocity for lower point, (m/s)

The passageway velocities varied and were generally less than the 0.20-m/s (0.66-ft/s) velocity of incipient sediment movement found in the first series of tests. For the 0.17-L/s (0.006-ft^3/s) discharge, the passageway velocity was 0.10 m/s (0.32 ft/s). The sand surface was close to the top of the tube (fig. 29b) and probably turbulence generated by water past the tube corrugations more readily reached the sand. Thus, a lower average velocity combined with the turbulence-caused sand movement. With increased passageway flow area, the effect of wall turbulence decreased and a higher average velocity [0.12 m/s (0.41 ft/s)] was necessary to move the sand. The last three discharges of the pyramid deposit test had a greater difference between the upper and lower points because partial dunes formed larger variances in the passageway flow areas, figures 29d, 29e, and 29f.

The lower point passageway velocities were believed more representative for the average velocity, producing incipient sediment movement. All these velocities were less than 0.20 m/s (0.66 ft/s) and thus the velocity of incipient sediment movement was considered in error. The explanation was that the pyramid deposit tests were done during a period of hours and sediment movement was detected by downstream dune movement. The earlier test was done during a period of minutes and sediment movement was detected by visual observation of sand grain movement.

Lengthwise Sediment Deposit

This was a more stringent test condition than that of the pyramid deposit. Sand was continually injected while there was a small water flow to determine whether the flow would be blocked.

A full-tube flow was established in the drain tubing with a test discharge of 0.20 L/s (0.007 ft³/s). Initially, sediment injection was rapid, but after a short time, sediment deposit built up and formed a small passageway near the top of the tubing. At this point, care was needed when placing sand into the sediment injection tube. If sediment injection was too fast, then sand blocked the passageway. The upstream hydraulic gradeline rose about 0.15 m (0.5 ft) until the pressure was sufficient to break the blockage. Thus, the sediment injection rate was governed by how fast sand was transported through the passageway.

Certainly, a large puncture would release enough sediment to block water flow through the tubing. However, a smaller puncture and quantity of sediment appeared to have a nonclogging tendency. A small passageway formed, provided high flow velocities, and transported sediment through the passageway to the end of the deposit. Here the flow velocity was less and the sediment dropped out at the end of the deposit. After 8900 cm³ of sand was injected, a lengthwise sediment deposit formed and sediment injection was stopped, figure 30a.

The discharge was progressively increased, resulting in a self-cleaning process for the deposit, figures 30b through 30e. For each discharge there was dune formation, which was more noticeable for the two larger discharges, figures 30d and 30e. At the 1.10-L/s (0.039-ft³/s) discharge, the deposit eroded down to the tubing invert.

Sediment motion was extremely slow. Short periods of observation disclosed no sand movement, but observations after 2 to 4 hours showed that sand had moved down the tube. After operating 18 hours at 0.20 L/s (0.007 ft³/s) discharge, the downstream end of the sediment deposit had not moved, figure 31b. However, some sand had eroded from the passageway and deposited a small dune-like hump on the thin-depthed downstream portion of the deposit, figure 30b. After operating 24 hours at a 0.40-L/s (0.014-ft³/s) discharge, the downstream end advanced 1 ft. Another 32 hours' operation with a 0.71-L/s (0.025-ft³/s) discharge produced a very pronounced dune formation, figure 30d, and the downstream end advanced 2 ft, figure 31d. Up to this stage, extension of the sediment deposit was dependent upon sand eroding from the passageway and being deposited at the end. However, for a 1.10-L/s (0.039-ft³/s) discharge, the sediment deposit lengthened by both erosion of the passageway and transport of small dunes along the tube bottom, figures 30e and 31g.

Similar to the pyramid deposit test, measurements were made of passageway depths, and velocities were computed for comparison with an incipient scouring velocity. The results are:

Q	t	D_u	D_l	V_u	V_l
0.20	18	0.22D	0.32D	0.16	0.09
0.40	24	.30D	0.55D	.18	.08
0.71	32	.40D	0.70D	.22	.11
1.10	23	.50D	1.00D	.26	.13

The variables and units of measure are as previously defined.

Dune formation was greater for the lengthwise sediment deposit than for the pyramid deposit and there was a greater difference between the upper- and lower-point velocities. These results show that using the upper point for comparison with incipient scouring velocity was wrong. Also, after further consideration, the fallacy was apparent; the high point of the dune was moving downstream.

For the 0.20-L/s (0.007-ft³/s) discharge, the lower-point passageway velocity was similar to the pyramid deposit. However, for the remaining three discharges, the lower-point velocity was less. Operation times for the lengthwise sediment deposit were greater than for the pyramid deposit. Thus, operation time appeared to be a factor affecting the value of an incipient scouring velocity. Determining when significant erosion had stopped during a test series was difficult. The incipient scour velocity was concluded to be 0.12 m/s (0.4 ft/s).

Hydraulic gradelines for the start and end of the four discharges showed that the sediment deposit resisted the flowing water, figure 32. The differential head ΔH, or the resistive effect of the sediment deposit, was measured between static head probes No. 5 and 6; see figure 32 table. Where the sediment deposit influenced the gradelines at probes No. 6 and 7, the gradeline was projected upstream from probes No. 8, 9, and 10. As the passageway was eroded and the flow area increased, resistance of the sediment deposit decreased from the start to the end of a given discharge.

Sediment Deposit in the 2DB Bend

Adjustments were made with the tailwater control gate to establish the one-fourth uniform depth for a discharge of 0.17 L/s (0.006 ft³/s) within the tube. Sand was then injected 0.6 m (2 ft) upstream from the bend test section. The sand was injected at a rate slow enough to maintain an open channel with a three-fourths, or smaller, flow depth upstream from the bend. After 2 hours of sediment injection, the sand had traveled into the bend. In the full-tube flow area, the sand settled and the depth of the sediment deposit increased. A passageway formed with velocities sufficient to transport sand to the downstream end of the sediment deposit, figure 33a. After 5 hours and the injection of 21 400 cm³ of sand, the sediment deposit was moving along the uphill leg of the bend, figure 33b. The flow was stopped for about 12 hours; a 0.17 L/s (0.006 ft³/s) discharge was again established to restart the test. After 2 hours' operation, the sand eroded from the passageway and had extended the sediment deposit almost to the end of the bend, figure 33c. The sand readily moved through the bend, in conjunction with a lowering of the upstream water surface, without blocking the waterflow. The discharge was continued for 65 hours, which extended the deposit 2.4 m (8 ft) downstream from the end of the bend, figure 33d. In figure 33d, the downstream end of the sediment deposit cannot be seen, but on the right side, sediment transportation can be seen occurring under open channel flow. The end of the sediment deposit was near static head probe No. 8, but the manometer reading had not changed from that adjusted at the beginning of the test.

The discharge was slowly increased to 0.74 L/s, (0.026 ft³/s), one-half flow depth for a 0.001 slope, without excessively disturbing the sand deposit. Readings from static head probes No. 8, 9, and 10, downstream from the sediment deposit, were used in setting the water surface. Upstream from the sediment deposit, the water surface was higher than the one-half flow depth because of flow resistance produced by the sediment deposit.

The sediment movement was more noticeable with the 0.74 L/s (0.026 ft³/s) discharge. Notice the increased passageway area of figure 33e over 33d. Within 2 hours after changing the discharge, dunes had formed on the smooth plain bed of the 2.4-m (8-ft) sediment deposit downstream from the bend. In 5 hours' operation, the downstream edge of the sediment deposited advanced 1.8 m (6 ft). About 12 hours later, the downstream edge had traveled 2.7 m (9 ft) to the tail box and was depositing in the box.

In 4 hours at the 0.74 L/s (0.026-ft³/s) discharge, an asymmetrical dune formation was observed along the entire length of the sediment deposit. From the front side of the tube, two adjacent dunes were seen, lower arrows of figure 33f. Using a mirror to observe the back side of the tube, a dune shape could be seen between those of the front side, upper arrow of figure 33f. This meandering of the sediment deposit along the tube was also present for the 1.10-L/s (0.039-ft³/s) discharge. Additional sand was flushed from the tube, the sediment deposit size decreased, and then the meandering sediment deposit was visible on the bottom of the tube, figure 34a. With continued operation at the 1.53-L/s (0.054-ft³/s) discharge and erosion of sand from the sediment deposit, the meandering shape of the sediment deposit disappeared, leaving symmetrical dune shapes, figure 34b. After 80 hours' operation at the 1.53-L/s (0.054-ft³/s) discharge, a dune movement of 0.02 m/h (0.05 to 0.1 ft/h) was observed for the free-surface flow condition in the straight tubing.

The 2DB bend sediment test was stopped after a total of 362 hours of operation. Very slowly the inflow valve was closed to gradually reduce waterflow through the tube and prevent surges in the pipe that might alter dune shapes. Water ponded in the pipe dripped from the tail box, thus preventing dune erosion as the tube drained. A slight meandering of the flow was evident in the shape of the dune crests, figure 34c. Static head probes No. 11 and 10 can be seen in the dunes, figure 34c.

Using the method described in the "Pyramid Sediment Deposit" section, a measure of passageway velocities was made for the sediment deposit in the 2DB bend. Results of the measurements are:

Q	t	D_u	D_l	V_u	V_l
0.17	65	0.2D	0.30D	0.15	0.09
0.74	124	.5D	0.75D	.17	.11
1.10	72	.6D	0.90D	.20	.13
1.53	101	.8D	1.00D	.20	.18

D = 105 mm (0.344 ft)

These velocities compare favorably to those of the pyramid and lengthwise sediment deposit tests. Evidently the bend did not noticeably influence the passageway velocities that are necessary to erode the sand.

The hydraulic gradelines for the start and end of the four test discharges, along with ΔH are shown in figure 35. Hydraulic gradelines from static head probes No. 1 through 5 were unaffected by the sediment deposit, but because probes No. 6 through 10 were at times covered or had sediment in their near vicinity, they have an unknown degree of inaccuracy. The ΔH was measured between static head probes No. 5 and 10, with an additional 9 mm (0.03 ft) subtracted to account for the 9.1-m (30-ft) distance between probes (9.1 m x 0.001 slope = 9 mm).

In figure 35, the lowermost hydraulic gradeline is for the first test discharge (0.17 L/s) and before injecting sand. After injecting sediment, the hydraulic gradeline (labeled 1S) at static head probe No. 5 rose 64 mm (0.21 ft). As operation continued, the erosion increased the passageway flow area, decreasing flow resistance of the sediment deposit. The gradeline (labeled 1E) dropped 34 mm (0.11 ft) at probe No. 5. At the end of the test, sand had traveled to static head probe No. 8, raising the 1E gradeline above the 1S gradeline at pr obe No. 7.

For discharge two 0.74-L/s, (0.026-ft³/s) manometer readings of uncovered probes No. 8, 9, and 10 were used to establish the one-half flow depth. From test start to end, erosion decreased the overall flow resistance of the sediment deposit. The upstream 2E hydraulic gradeline was lower than the 2S gradeline. Movement of the sediment deposit to the tail box raised the 2E gradeline above the 2S gradeline for probes No. 8, 9, and 10.

In setting flow depths for test discharges 1 and 2, static head probes downstream from the sediment deposit could be used. However, at the end of test discharge 2, the sediment deposit had reached the tail box. At static head probe No. 10, the gradeline rose approximately 3 mm (0.01 ft) during the test. The sediment deposit influenced the control of water surface elevation for the remaining two test discharges.

The third test discharge of 1.10 L/s (0.039 ft³/s) was adjusted by gradually increasing the discharge without changing the tailwater control gate. After each increased discharge, the flow depth indicated by static head probe No. 10 was compared to that of figure 13, and was within 6 mm (0.02 ft). Upon reaching the 1.10-L/s (0.039-ft³/s) discharge, probe No. 10 indicated a 70-mm (0.231-ft) water depth. From figure 13, the flow depth should be 66 mm (0.218 ft), but considering that at the end of test discharge 2, the sediment deposit raised the flow depth 3 mm (0.01 ft) (66 + 3 = 69-mm flow depth), the above flow conditions were accepted. There was a lowering of the hydraulic gradeline from the start to the end of the discharge, see curves 3S and 3E of figure 35.

A 1.53-L/s (0.054-ft³/s) discharge, between three-fourths flow depth and full pipe flow (fig. 13), required adjustments of the tailwater control gate to establish an 85-mm (0.280-ft) depth at probe No. 10. The 4E hydraulic gradeline was slightly lower than the 4S gradeline, figure 35.

Operation time was 362 hours for the 2DB bend sediment test and sand was still exiting from the tubing. In the earlier sedimentation tests, equilibrium was judged to have occurred. However, as each sediment test was made, a longer test time was used. Experience showed that waiting for equilibrium of a sediment deposit was very slow and time consuming.

Sedimentation tests had been made for free-surface and full-tube flow conditions of straight tubing and for full-tube flow of the 2DB bend. The test results were believed applicable for an above-grade bend. For instance, with a 2DA bend there would be full-tube flow upstream from the bend midpoint. Sediment would travel along the straight tubing similar to the lengthwise deposit tests and along the uphill leg of the 2DA bend similar to the uphill leg of the 2DB bend. Then downstream from the 2DA bend, sediment would move, depending upon free-surface or full-tube flow conditions. Therefore, the testing program formulated prior to the study was believed accomplished and no further tests were made.

One criticism was that the nonperforated laboratory tubing allowed different sediment behavior than a perforated field drain. While the nonclogging tendency occurred in the 2DB bend laboratory tests, it may not occur in the field. The argument was that water could flow through the perforations into the gravel envelope, downstream through the gravel envelope, and allow sediment to block waterflow in the bend. However, in this event, the discharge through the gravel envelope would be small, and not very much sediment would be moved along the tubing to where water was exiting through the perforations. It is believed this condition would be representative of almost no flow at all through the drain and probably field drains do not operate very long at this condition.

GPO 846 - 837

ABSTRACT

Laboratory tests were made with an 18-m (60-ft) long, 100-mm (4-in) diameter, nonperforated plastic drain tube. Probes for measuring the static head were 2.4-mm (3/32-in) diameter and placed at 1.8-m (6-ft) intervals along the tube. Tests were made for full-tube flow and free-surface flow at 0.001, 0.005, 0.01, and 0.02 tube slopes. The test results are given in graphs of average velocity and discharge versus uniform depth. Manning's *n* was approximately 0.016. Grade deviations were studied with bends. Four bends, 2.4 m (8 ft) long, with one- and two-tube diameter offsets above and below grade, were tested. There was a significant rise in the hydraulic gradeline upstream from the bend only with bends above grade and for conditions of free-surface flow. A fine, uniform 0.2-mm mean diameter sand was used for sedimentation tests. For flow conditions with a 0.001 slope and a two-diameter tube offset bend below grade, the sediment did not prevent waterflow through the bend.

ABSTRACT

Laboratory tests were made with an 18-m (60-ft) long, 100-mm (4-in) diameter, nonperforated plastic drain tube. Probes for measuring the static head were 2.4-mm (3/32-in) diameter and placed at 1.8-m (6-ft) intervals along the tube. Tests were made for full-tube flow and free-surface flow at 0.001, 0.005, 0.01, and 0.02 tube slopes. The test results are given in graphs of average velocity and discharge versus uniform depth. Manning's *n* was approximately 0.016. Grade deviations were studied with bends. Four bends, 2.4 m (8 ft) long, with one- and two-tube diameter offsets above and below grade, were tested. There was a significant rise in the hydraulic gradeline upstream from the bend only with bends above grade and for conditions of free-surface flow. A fine, uniform 0.2-mm mean diameter sand was used for sedimentation tests. For flow conditions with a 0.001 slope and a two-diameter tube offset bend below grade, the sediment did not prevent waterflow through the bend.

ABSTRACT

Laboratory tests were made with an 18-m (60-ft) long, 100-mm (4-in) diameter, nonperforated plastic drain tube. Probes for measuring the static head were 2.4-mm (3/32-in) diameter and placed at 1.8-m (6-ft) intervals along the tube. Tests were made for full-tube flow and free-surface flow at 0.001, 0.005, 0.01, and 0.02 tube slopes. The test results are given in graphs of average velocity and discharge versus uniform depth. Manning's *n* was approximately 0.016. Grade deviations were studied with bends. Four bends, 2.4 m (8 ft) long, with one- and two-tube diameter offsets above and below grade, were tested. There was a significant rise in the hydraulic gradeline upstream from the bend only with bends above grade and for conditions of free-surface flow. A fine, uniform 0.2-mm mean diameter sand was used for sedimentation tests. For flow conditions with a 0.001 slope and a two-diameter tube offset bend below grade, the sediment did not prevent waterflow through the bend.

ABSTRACT

Laboratory tests were made with an 18-m (60-ft) long, 100-mm (4-in) diameter, nonperforated plastic drain tube. Probes for measuring the static head were 2.4-mm (3/32-in) diameter and placed at 1.8-m (6-ft) intervals along the tube. Tests were made for full-tube flow and free-surface flow at 0.001, 0.005, 0.01, and 0.02 tube slopes. The test results are given in graphs of average velocity and discharge versus uniform depth. Manning's *n* was approximately 0.016. Grade deviations were studied with bends. Four bends, 2.4 m (8 ft) long, with one- and two-tube diameter offsets above and below grade, were tested. There was a significant rise in the hydraulic gradeline upstream from the bend only with bends above grade and for conditions of free-surface flow. A fine, uniform 0.2-mm mean diameter sand was used for sedimentation tests. For flow conditions with a 0.001 slope and a two-diameter tube offset bend below grade, the sediment did not prevent waterflow through the bend.

REC-ERC-78-2
Zeigler, E. R.
HYDRAULIC LABORATORY MANNING'S *n* AND GRADE DEVIATION STUDY FOR 4-INCH-DIAMETER NONPERFORATED, CORRUGATED PLASTIC DRAIN TUBING
Bur Reclam Rep REC-ERC-78-2, Div Res, Feb 1978, Bureau of Reclamation, Denver, 55 p, 37 fig, 3 app.

DESCRIPTORS–/ *subsurface drains/ hydraulics/ fluid flow/ steady flow/ subcritical flow/ *discharge (water)/ *flow resistance/ hydraulic gradient/ *water surface profiles/ *bends/ sedimentation/ deposition/ erosion/ bed movements
IDENTIFIERS–/ nonperforated, corrugated plastic drain tubing

COSATI Field/Group 13K COWRR: 1311

REC-ERC-78-2
Zeigler, E. R.
HYDRAULIC LABORATORY MANNING'S *n* AND GRADE DEVIATION STUDY FOR 4-INCH-DIAMETER NONPERFORATED, CORRUGATED PLASTIC DRAIN TUBING
Bur Reclam Rep REC-ERC-78-2, Div Res, Feb 1978, Bureau of Reclamation, Denver, 55 p, 37 fig, 3 app.

DESCRIPTORS–/ *subsurface drains/ hydraulics/ fluid flow/ steady flow/ subcritical flow/ *discharge (water)/ *flow resistance/ hydraulic gradient/ *water surface profiles/ *bends/ sedimentation/ deposition/ erosion/ bed movements
IDENTIFIERS–/ nonperforated, corrugated plastic drain tubing

COSATI Field/Group 13K COWRR: 1311

REC-ERC-78-2
Zeigler, E. R.
HYDRAULIC LABORATORY MANNING'S *n* AND GRADE DEVIATION STUDY FOR 4-INCH-DIAMETER NONPERFORATED, CORRUGATED PLASTIC DRAIN TUBING
Bur Reclam Rep REC-ERC-78-2, Div Res, Feb 1978, Bureau of Reclamation, Denver, 55 p, 37 fig, 3 app.

DESCRIPTORS–/ *subsurface drains/ hydraulics/ fluid flow/ steady flow/ subcritical flow/ *discharge (water)/ *flow resistance/ hydraulic gradient/ *water surface profiles/ *bends/ sedimentation/ deposition/ erosion/ bed movements
IDENTIFIERS–/ nonperforated, corrugated plastic drain tubing

COSATI Field/Group 13K COWRR: 1311

REC-ERC-78-2
Zeigler, E. R.
HYDRAULIC LABORATORY MANNING'S *n* AND GRADE DEVIATION STUDY FOR 4-INCH-DIAMETER NONPERFORATED, CORRUGATED PLASTIC DRAIN TUBING
Bur Reclam Rep REC-ERC-78-2, Div Res, Feb 1978, Bureau of Reclamation, Denver, 55 p, 37 fig, 3 app.

DESCRIPTORS–/ *subsurface drains/ hydraulics/ fluid flow/ steady flow/ subcritical flow/ *discharge (water)/ *flow resistance/ hydraulic gradient/ *water surface profiles/ *bends/ sedimentation/ deposition/ erosion/ bed movements
IDENTIFIERS–/ nonperforated, corrugated plastic drain tubing

COSATI Field/Group 13K COWRR: 1311